The Pennsylvania State University
The Graduate School

AN INTERCOMPARISON OF TROPOSPHERIC OZONE DERIVED FROM TWO AURA INSTRUMENTS

A Thesis in
Meteorology
by
David Doughty

Submitted in Partial Fulfillment
of the Requirements
for the Degree of

Master of Science

December 2009

The thesis of David Doughty was reviewed and approved* by the following:

Anne Mee Thompson
Professor of Meteorology
Thesis Advisor

Eugene Clothiaux
Professor of Meteorology

Derek Lampkin
Professor of Geography

Hans Verlinde
Professor of Meteorology
Chair of Meteorology Graduate Program

*Signatures are on file in the Graduate School.

Abstract

In situ ozonesonde measurements from the IONS-06 (NASA's INTEX [Intercontinental Chemical Transport Experiment] Ozonesonde Network Study) 2006 intensive field campaign are compared with two estimates of ozone derived from Aura satellite retrievals taken daily in the same period (April-May 2006). The domain of validation is northwest North America, where gradients in column ozone can present technical challenges to precise ozone measurement. One estimate is based on mapping stratospheric ozone to forward trajectories for global coverage, then subtracting integrated stratospheric column ozone from the total column ozone to derive tropospheric column ozone. The other technique uses total column ozone and stratospheric profiles in an assimilation into a chemical-transport model that provides three-dimensional ozone fields. Although both retrieval techniques approximate variability observed in day-to-day in-situ measurements, it is found that the assimilation yielded tropospheric ozone column values 1.9% less than ozonesondes, and tropospheric ozone residual tropospheric ozone columns were 15.7% less than ozonesondes. Additionally, profiles from the assimilation method showed persistent high bias from 300 to 200 hPa, that partially cancelled with negative biases in the lower troposphere, so apparent elevated accuracy of the assimilation method is to some degree a consequence of compensating errors within the troposphere. Finally, cases are examined to better understand potential factors that may be the performance of the assimilation, especially with regards to meteorological conditions. Analysis of cases suggest that some errors in the upper troposphere are due to complex synoptic conditions, but not all error can be explained by dynamics.

Table of Contents

List of Figures

List of Tables

Acknowledgments

First, I want to thank my advisor Anne Thompson for all her hard work, encouragement, and criticism. Without her, who knows where I would be? I thank my committee, Derrick Lampkin and Eugene Clothiaux for helping bring this thesis out of the murky depths. I cannot thank my labmates enough for all the support and advice. Thanks to Ivanka Stajner, Mark Schoeberl, and Sam Oltmans who who offered advice on data quality and supplied the data products, and to all those who were involved in the IONS-06 campaign. Finally, I want to thank my parents for their prayers and support, as well as a certain chess grand master. Without you, I'd have been lost a long time ago.

Chapter 1

Introduction

1.1 Importance of Atmospheric Ozone

Because atmospheric ozone can have a great impact on quality of life, it is important that it be studied and understood. Ninety percent of all the ozone in the atmosphere is found in the stratosphere, where it absorbs much of the ultraviolet radiation at wavelengths below 290 nm. Most prevalent in the stratosphere, ozone at all levels absorbs harmful ultraviolet radiation (Fig. 1.1). Although ozone in the troposphere can have a slight warming effect, it can also attack the lungs of humans and animals, and can have deleterious effects on plants which can impact agricultural economics (Fiscus et al., 2005).

Atmospheric ozone has been studied since the late 1800's, but the ability to understand the distribution of ozone increased greatly after G.M.B. Dobson designed an improved ultraviolet (UV) spectrometer which allowed determination of total column ozone from the ground (Dobson, 1931). This instrument worked by measuring differential absorption of ultraviolet light between strong and weak bands to determine the total amount of ozone between the sensor and the sun. Dobson (1968) notes that this system offered increased durability, accuracy, and simplicity over previous differential absorption methods such as the Féry spectrograph. By 1968, over 100 of these spectrometers had been produced. Today, Dobson Spectrometers still provide very accurate validation for satellite derived total ozone column amounts, although in many places, they are being replaced by the more advanced Brewer spectrometer.

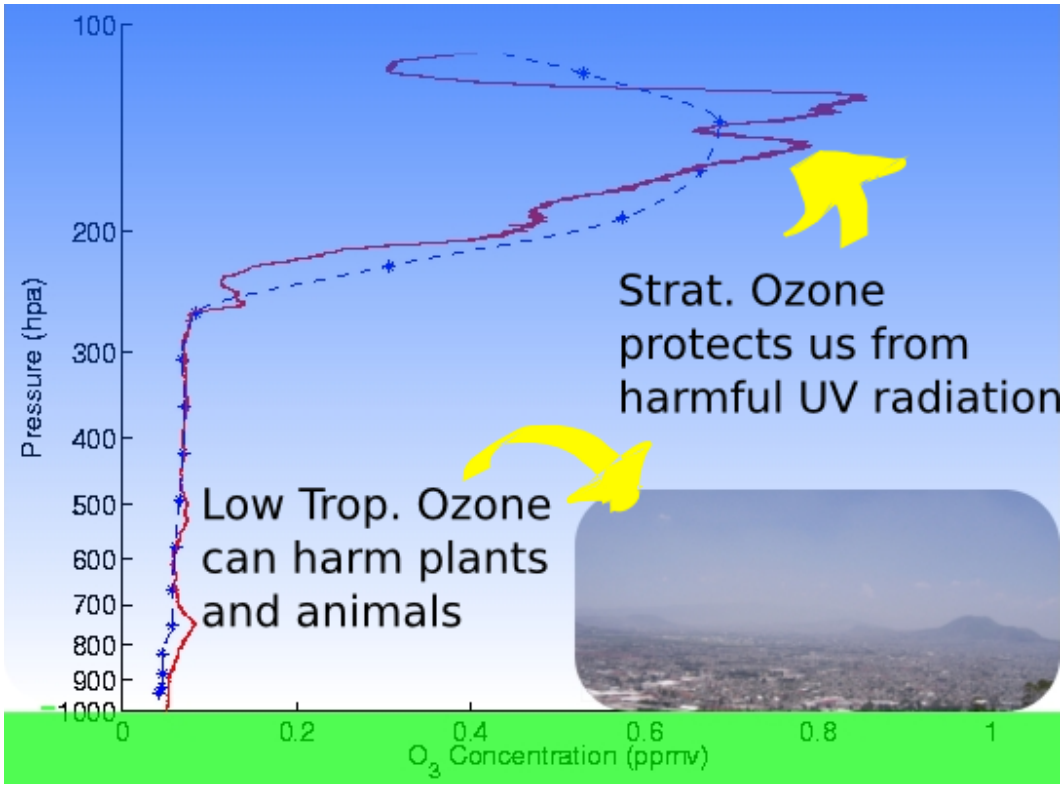

Figure 1.1. In-situ ozone profiles (solid red line) and satellite retrieval (dashed blue line) Note elevated ozone concentrations in the stratosphere and lower concentrations in the troposphere.

Gotz et al. (1934) noted that the surprising increase in the ratio in intensities of zenith radiation (at the two wavelengths used in the Dobson spectrometer) when the sun was at low angles. This happened because at low sun angles, sunlight scattered in the high stratosphere dominated the radiation recieved by the detector. This "turning back" (umkehr means 'to turn back' in German) of the relative absorption curve allowed average ozone height in the atmosphere to be estimated (Gotz et al., 1934). Further improvements in ozone knowledge and computing power would eventually allow this method to be used for determination of ozone profiles (Dobson, 1968). While this technique is useful for depletion studies, it is not suitable for measurement of tropospheric ozone because only 10% of ozone is in the troposphere. (Fig. 1.1).

In the 1960s Brewer and Milford (1960) pioneered the development of the ozonesonde, a device that chemically measures ozone in-situ. Generally launched

with a radiosonde for telemetry, and pressure and humidity measurements, ozone retrievals up to the middle stratosphere are possible. Komhyr (1969) and others developed the Electrochemical Concentration Cell (ECC) ozonesonde, which improved upon the Brewer-Milford technique, and is commonly used in many locations around the world today, including the sites that will be examined in this thesis.

Because ozonesondes and Dobson spectrometers have been in use for decades, significant time series exist at two US sites since the 1970s, as well as at several other stations around the world. Table 1.1 lists several locations where total column ozone and ozone profiles have been measured since the 1970's. A full listing of most ozone monitoring sites can be found at the World Ozone and Ultraviolet Data Center, www.woudc.org. These sites do not represent full global coverage, e.g. only four North America locations have long time-series data available, and the remainder are biased toward the Northern Hemisphere by approximately a three to one ratio.

Station	Period	Type
Wallops Island,USA	1970-2009	Dobson*
Wallops Island, USA	1970-2009	ECC
Boulder, USA	1970-2009	Dobson*
Boulder,USA	1979-2009	ECC
Edmonton, CAN	1979-2009	ECC
Edmonton, CAN	1984-2004	Brewer*
Churchill, CAN	1970-2005	Dobson*
Churchill, CAN	1970-2009	ECC
Hohenpeissenberg, DEU	1970-2009	Brewer-Mast
Sapporo, JPN	1970-2009	Carbon-Iodine
Sapporo, JPN	1970-2009	Dobson*

Table 1.1. Locations of several long-term ozone monitoring sites

Scientists would have to wait for the launch of the Nimbus satellite in 1970 for long-term global ozone column measurements. Sensors on Nimbus had the capability to measure total column ozone values, from space, via differential absorption

of ultraviolet light using a method similar to the Dobson and Brewer spectrometers. This provided global ozone data, and similar measurements have now been made for the past 40 years. As a result, scientists have a long term record of total column ozone(Fig. 1.2, which offers a consistent calibration because subsequent ozone satellites (Nimbus-7, EarthProbe, and Aura) also carried instruments that could make the same measurements.

In the late 1970s, the Stratospheric Aerosols and Gases Experiment(SAGE) satellite allowed remote sensing of stratospheric ozone profiles. SAGE (Mccormick et al., 1979) was a solar occultation satellite that used changes in solar spectra as the sun set to measure stratospheric ozone. Fishman et al. (1990) subtracted SAGE stratospheric column ozone from Total Ozone Mapping Spectrometer (TOMS) total column ozone to estimate the tropospheric ozone from space. This was the first satellite measurement of tropospheric ozone, called the Tropospheric Ozone Residual (TOR), but it was limited to multi-month climatologies due to the relatively few number of SAGE profiles (Fishman and Brackett, 1997), and because stratospheric measurements did not resolve the tropopause well. Twenty-year TOR amounts can be seen in Fig. 1.3. The frequency of tropospheric ozone residuals has been improved by incorporating limb sounding measurements from the Microwave Limb Sounder (MLS) and Ozone Monitoring Instrument (OMI) onboard NASA's AURA satellite because they are on the same platform retrieving daily images. Nonetheless, this method has several difficulties retrieving tropospheric ozone. For example, MLS retrieves one profile every 165 km along the suborbital track (Waters et al., 2006). This covers much less of the earth's surface than OMI, which has a swath width of 2600 km and a resolution of 13 by 28 kilometers(Levelt et al., 2006). To solve this problem, stratospheric data is typically time-aggregated, usually by mapping it to atmospheric variables that are better resolved over the earth's surface (Schoeberl et al., 2007).

Data assimilation takes the tropospheric ozone residual method one step further by using satellite measurements to improve the output of models. This method offers an improvement over ozone residual measurements because it includes effects of cloud transport and ozone photochemistry (Stajner et al., 2008). It is limited by the ability of models to resolve atmospheric features, especially in the upper troposphere and lower stratosphere. Nevertheless, Schoeberl et al. (2007) note that

"Full 3-d chemical assimilation is probably the ultimate solution since modern assimilation techniques better handle meteorological and instrument uncertainties."

1.2 Outline

The goal of this study is to examine the performance of modern ozone residual and data assimilation methods for quantifying tropospheric ozone abundances. Before beginning the analysis, we examine the Aura satellite and its instruments, as well the techniques behind the Trajectory-Enhanced Tropospheric Ozone Residual (Schoeberl et al., 2007) and an assimilation of AURA data into GEOS-4 (Stajner et al., 2008). We look deeper into the advantages and limitations of each of these methods by comparing tropospheric ozone from the assimilation and residual to in-situ measurements from ozonesondes. We present a statistical picture of the performance of both data products.

To better charactarize the performance of data assimilation in retrieving ozone profiles, we also compare profile retrievals from this method to those from ozonesondes. Profile differences allow for examination of the factors contributing to inaccuracies in data assimilated tropospheric ozone, and also aid in identification of altitudes where the assimilation has particular difficulty estimating atmospheric ozone.

To illustrate retrieval method difficulties, we consider three case studies. Two cases consist of periods when significant errors in tropospheric ozone cause erroneous upper troposphere ozone estimates in the satellite-derived data products, and the third is a day when the assimilation has an accurate retrieval of ozone up to the top of the troposphere. Analysis of these case studies allow us to examine the link between dynamic conditions and significant errors in both of the satellite data products.

These three case studies will present a picture of how both satellite-derived ozone data products perform in the Pacific Northwest during a complicated dynamical regime in springtime. This aids in determining the value of these new data products for scientific use.

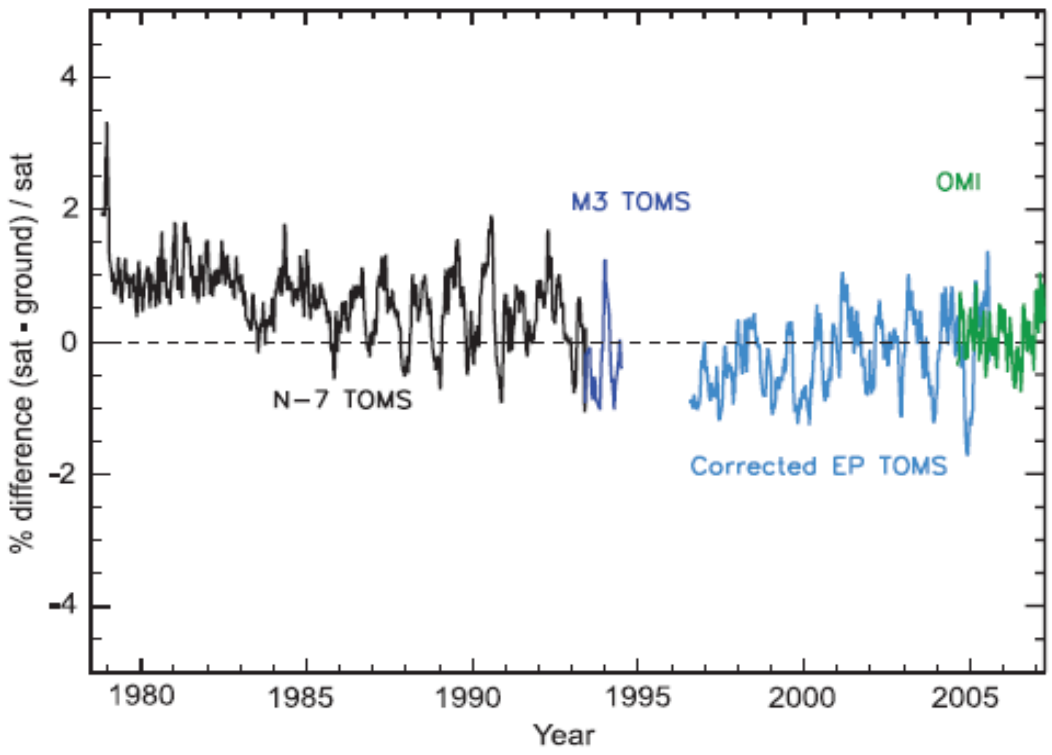

Figure 1.2. TOMS time series shows continuity over four satellites and over thirty years of nearly continuous records. Comparisons are with an ensemble of 30 Northern Hemisphere Dobson Spectrometer stations (McPeters et al., 2008).

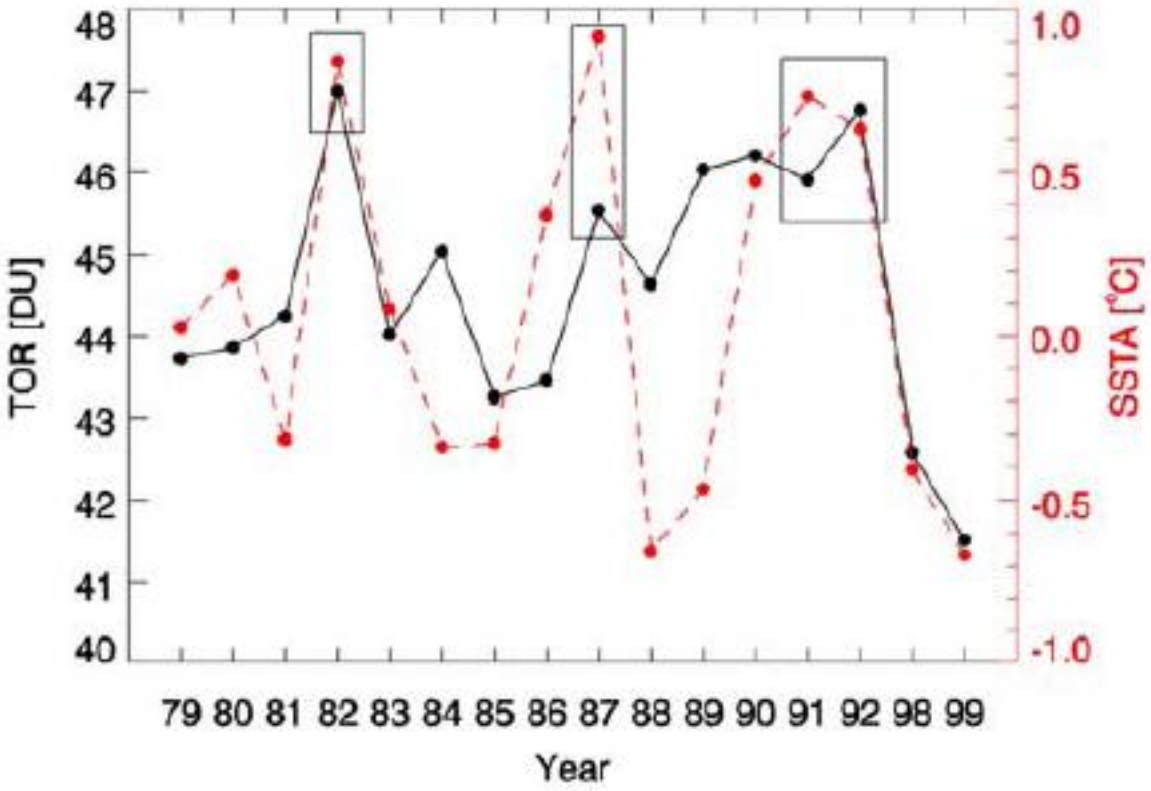

Figure 1.3. Time-series of annually averaged tropospheric ozone residuals over India, shown in black compared with sea surface temperature anomalies in the Western Pacific (a proxy for ENSO), shown in red (Fishman et al., 2005).

Chapter 2

Datasets and Methodology

2.1 Aura Datasets

This study examines data derived from the Aura satellite. Launched on July 15, 2004, Aura orbits at a height of 705 km, and has an orbital period of 98.8 minutes. It is a sun synchronous, polar-orbiting satellite, which means that it has a fixed position relative to the sun, crossing the equator at 1:45 PM local time on its ascending node as it circles the Earth 14 times per day (Levelt et al., 2006; Waters et al., 2006). It is one of five NASA satellites that fly in formation in what is referred to as the "A-Train", making complementary measurements of the Earth's atmospheric composition. There are four instruments onboard Aura: the Ozone Monitoring Instrument (OMI), the Microwave Limb Sounder (MLS), the Tropospheric Emission Spectrometer (TES), and the High Resolution Dynamic Limb Sounder (HRDLS). The data in this thesis are based upon measurements by the OMI and MLS.

OMI was designed to measure important trace gases, including ozone, with a small footprint and daily global coverage. OMI's nadir pointing telescope (Fig. 2.1) has a 13 km by 28 km footprint, and swath width of of each scan is 2600 km which allows daily global coverage. The three measurement channels cover a range 270 to 500 nm with a spectral resolution of around 0.5 nm. OMI data are calibrated once per day by solar observation. Additional details about instrument performance and operation can be found in Levelt et al. (2006).

Data from OMI is used in two algorithms to obtain total column ozone: Ver-

sion 8 of the Total Ozone Mapping Spectrometer (TOMS) algorithm and Differential Optical Absorption Spectroscopy (DOAS). Because various versions of the TOMS algorithm have been used since the 1970s, OMI-TOMS provides continuity with older satellite-based ozone instrument measurements (McPeters et al., 2008). Measurements from six wavelengths in the ultraviolet parts of the electromagenetic spectrum are put into to the TOMS algorithm. Two of the chanels are used to retrieve ozone and the remaining four are used to improve data quality. McPeters et al. (2008) compared TOMS ozone retrievals with Dobson and Brewer spectrometer measurements and found that OMI-TOMS total column ozone averaged 0.4% higher than the ground stations; Balis et al. (2007) found agreement of better than 1% between OMI-TOMS and ground stations.

DOAS obtains total column ozone by including slant column data and accounting for sun-surface-satellite geometry and other factors in its analysis (McPeters et al., 2008). This ozone retrieval method is not used for either of the tropospheric ozone products examined in this thesis, but accuracy information is included for completeness. DOAS comparisons with ground spectrometers by McPeters et al. (2008) found offsets of 1.1%, with a seasonal dependence of $\pm 2\%$ and a significant dependence on solar zenith angle. Comparison of OMI-DOAS to surface spectrometers by Balis et al. (2007) showed agreements of better than 2%.

MLS uses five radiometers to make radiance measurements between 118 GHz and 2.5 THZ to retrieve profiles of temperature, pressure, and atmospheric trace gases (Waters et al., 2006). MLS scans in the direction of orbital motion (Fig. 2.1), retrieving individual profiles every 165 km along its track. The vertical resolution is 3 km, and approximate horizontal resolution is 300 km in the Upper Troposphere/Lower Stratosphere (UTLS) region. Precision ranges from 20% at the 215 hPa level to 3-5% in the stratosphere (Froidevaux et al., 2008; Boyd et al., 2007).

Both the OMI and MLS measurements have limitations. OMI only measures the total amount of ozone in a column of air, whereas MLS measurements have a very limited coverage area and only resolve the stratosphere and upper troposphere. While these measurements are useful for studying the global distribution of ozone and changes of stratospheric ozone, extracting tropospheric ozone from these measurements represents a more difficult problem. Several methods have been developed to retrieve tropospheric ozone from satellite measurements.

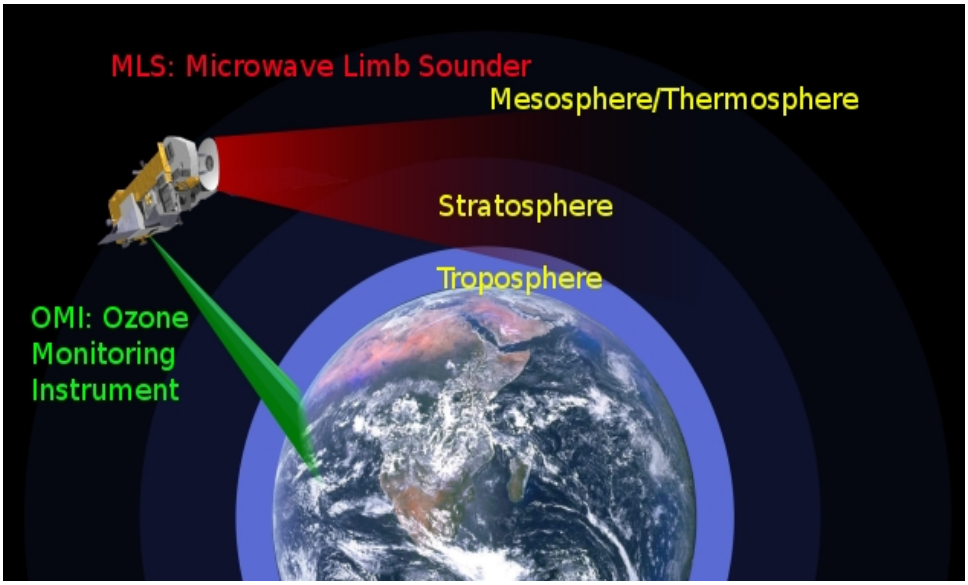

Figure 2.1. Illustration of the capabilities of OMI and MLS onboard the AURA satellite. OMI, pictured in green, is a nadir pointing instrument that provides total column values of ozone and other atmospheric constituents. MLS, pictured in red, is a limb instrument that looks in front of AURA and provides stratospheric profiles of ozone and other atmospheric constituents.

In its simplest form, a tropospheric ozone residual is obtained by subtracting stratospheric column ozone from total column ozone to yield tropospheric column ozone. The first tropospheric ozone residuals used the TOMS algorithm for total ozone and SAGE profiles to estimate the stratospheric column ozone (Fishman et al., 1990), and offered monthly and seasonal tropospheric column ozone amounts. This method has been modified by using newer satellite observations, with higher spatial and temporal resolution, and mapping techniques to extend stratospheric profiles, which usually have narrow coverage, to a larger area of the Earth. This means that tropospheric column ozone residual methods are viable for retrieving daily tropospheric ozone. A list of selected tropospheric ozone residual methods can be seen in Table 2.1.

This study examines the Trajectory-enhanced Tropospheric Ozone Residual (TTOR) (Schoeberl et al., 2007). TTOR (version 1.4) uses six-day isentropic forward trajectories to spread MLS measurements over Earth's surface. Then the MLS forward trajectories and OMI measurements are interpolated to a 1.25 by 1

Technique	Principles Involved	Reference
Tropospheric Ozone Residual (TOR)	Subtract SBUV SCO from TOMS TCO	Fishman et al (1987)
Trajectory-Enhanced TOR	Map TOR to forward trajectories	Schoeberl et al. (2007)
TOR with Convective Cloud Differential	Calibrate TOR with OMI CCD	Ziemke et al (2007)
PV mapped TOR	MAP TOR to PV for global coverage	Yang et al. (2007)
OMI Estimation	Optimal Estimation	Liu et al. (2009)
Multi-Sensor Upper Troposphere Ozone	TES ozone and GOES water vapor	Felker et al. (Submitted)
OMI/MLS Assimilation into GEOS-4	GEOS-4, TOC and Strat. Profile	Stajner et al. (2008)

Table 2.1. Several modern methods for obtaining tropospheric column ozone from satellite measurements. Acronym Definitions can be found in appendix A

degree grid. Finally, stratospheric column ozone is subtracted from total column ozone to retrieve tropospheric column ozone. This method offers two advantages over the standard tropospheric ozone residual. First, the use of the Microwave Limb Sounder allows daily profiles to be analyzed, and second, the trajectory mapping allows potentially more accurate estimates of global tropospheric column ozone.

The Aura Assimilation, hereafter Aura-ASM, uses MLS ozone profiles and OMI total ozone columns to improve the output of the GEOS-4 data assimilation system. Aura-ASM is similar to trajectory mapping because it uses assimilated meteorological fields along with a general circulation model (GCM) (Bloom et al., 2005). Unlike trajectory mapping, it also uses these fields to drive a photochemical model that accounts for ozone production, loss, and deposition during transport (Stajner et al., 2008). This product provides ozone mixing ratios at 55 vertical layers throughout the atmosphere on a horizontal grid of 1.25° by 1° grid. Twelve of these layers typically lie in the troposphere (Stajner et al., 2008).

2.2 In-Situ Ozonesondes

In-situ ozone profiles are measured using Electrochemical Concentration Cell(ECC) ozonesondes. They utilize the reaction

$$2KI + O_3 + H_2O \rightarrow 2KOH + I_2 + O_2$$

The I_2 undergoes further reactions, eventually yielding two electrons for each ozone molecule. The electric current is measured in proportion to the number of ozone

molecules, and a modified radiosonde sends ozone partial pressure measurements to a ground station, along with radiosonde measurements of pressure, temperature, humidity, and sometimes winds (En-Sci 1999). The precision of the ozonesondes in the troposphere is 5-10% (Smit et al., 2007). ECC ozonesondes have been utilized since the 1960s (Komhyr, 1969), and a continuous record exists at two US locations and several sites in Canada, Europe, and Japan. As noted in the previous chapter, coverage of the entire atmosphere with ozonesondes is not logistically possible, although there have been attempts to extrapolate sonde measurements during intensive campaigns to regional scales by trajectory mapping (Tarasick et al., Submitted).

2.3 Site Selection

Aura-derived tropospheric ozone was compared to ozonesondes launched during spring 2006 at four sites in the Pacific Northwest region of the US and Canada. This period was selected because an intensive ozonesonde campaign, called IONS-06 was conducted during the spring of 2006 that achieved the near-daily launch times required for an in-depth time-series analysis. Data from the IONS-06 campaign can be found at http://croc.gsfc.nasa.gov/intexb/ions06.html. Spring months were chosen because, during the Spring, the top of the troposphere is dynamically complex and can cause difficulty in some models and satellite ozone retrievals.

Four locations were selected from the Pacific Northwest because they are geographically close, yet topographically diverse. Bratts Lake, SK, is located on the plains in southern Canada; Kelowna, BC, is located in the Cascade mountains; Richland, WA is located on the slopes of the Cascade Mountains; and Trinidad Head, CA, is adjacent to the Pacific Ocean. Refer to Fig. 2.2 for a map of analysis sites, along with approximate sizes of colocated assimilation model grid-squares.

2.4 Methods

The first step in evaluating the accuracy of the TTOR and Aura-ASM ozone retrievals is to calculate integrated tropospheric ozone. This is the only tropospheric data that the TTOR product supplies and is also a good first metric for the perfor-

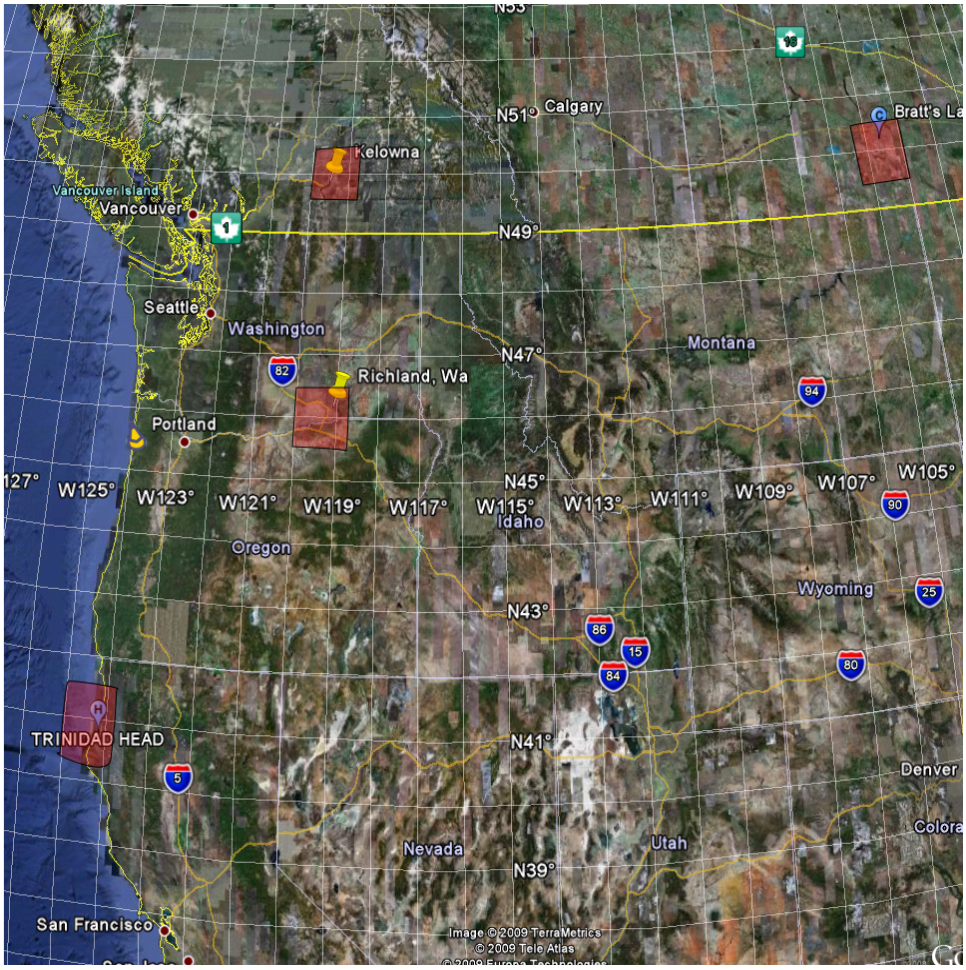

Figure 2.2. The four locations whose data were analyzed in this thesis. From lower left to upper right, Trinidad Head, CA; Richland, WA; Kelowna, BC; Bratts Lake, SK. Red boxes show approximate sizes and locations of GEOS-4 grid squares.

mance of Aura-ASM, where tropospheric column ozone is obtained by integrating ozonesonde measurements from the surface to the tropopause. Therefore, the location of the tropopause (top of the troposphere) is important because it affects the outcome of the integration. Moreover, the forcings that affect ozone concentration are very different between the stratosphere and troposphere, and so the forcings that effect ozone will vary depending on the location of the tropopause. The stratospheric ozone cycle is affected primarily by photochemistry, and large scale, slowly varying (on the order of months) transport, whereas tropospheric ozone is influenced by synoptic-scale transport, photochemistry, surface produc-

tion and destruction, and lightning (Thompson et al., 1999, 2007). Because of the different forcings, ozone concentrations in the stratosphere are much higher than ozone in the troposphere so deciding where the troposphere ends has a great impact on estimated tropospheric column ozone.

There are several tropopause definitions that rely on differences in potential vorticity or lapse rate between the troposphere and stratosphere. Other methods rely on the increase in ozone concentration at the tropopause. Dougherty (2008) found that methods based on ozone gradients, or that started from the stratosphere and decended toward the troposphere to a low ozone cutoff, were most effective. In this study, we select a 200 hPa tropopause in the integration of tropospheric ozone measurements and estimates. While this has the potential to capture some stratospheric ozone, it also avoids biasing retrieval accuracy by tropopause height. For example, equatorial locations have a higher tropopause height than subtropical and polar locations. Therefore, if a model has problems at a certain height that is above the tropopause in southern locations but below in northern locations, or that is above the tropopause during the winter but below during the summer, calculated tropospheric amounts may be biased by tropopause height. Thus a static height was needed. At midlatitudes in springtime, 200 hPa is a standard height, and is often close to the tropopause claculated by other methods (see Fig. 3.6 and 3.7). Finally, this height has been used in other validation studies (Schoeberl et al., 2007; Stajner et al., 2008). To extract tropospheric ozone column from the AURA-ASM data product, ozone mixing ratios were linearly interpolated to regular levels and integrated using the equation

$$.7891 \int_{p_t}^{p_s} \mu \cdot dp$$

as described in Stajner et al. (2008). In this equation μ is the ozone mixing ratio in Parts Per Million by Volume (PPM_{bv}), p is the pressure, p_t is the tropopause pressure, p_s is the surface pressure in hPa. For ozonesonde data, we applied the equation

$$26.93 \int_{z_t}^{z_s} \frac{p(z)\mu_z}{T(k)} dz$$

where p(z) is the pressure at a height z, z_t is the tropopause height, z_s is the surface

height, $T(k)$ is the temperature in degrees kelvin, and μ is the ozone concentration in PPM_{bv} (Dougherty, 2008). Once tropospheric ozone column estimates were produced, we calculated errors and percent differences for each day of the study period.

In addition to the tropospheric ozone column, we also examined the performance of Aura-ASM ozone profiles. The Aura-ASM product provides average ozone concentration between two pressure levels. we averaged ozonesonde measurements over these pressure levels to compare to Aura-ASM.

Finally, we developed case study periods to understand irregularities in the performance of the Aura-ASM ozone estimation method.

Chapter 3

Initial Results and Statistics

This chapter will examine time-series data from four IONS-06 locations. First, we will show the time-series plots, residual histograms, and mean percent differences of tropospheric column ozone to understand generally how TTOR and Aura-ASM resolve tropospheric ozone during the study period. Then, we examine profiles from Aura-ASM to better understand factors that affect its performance.

3.1 Ozone Overall Statistics

We compared both TTOR and Aura-ASM data products to ozonesondes during the IONS-06 study in the spring of 2006. Figures 3.1 and 3.2 show this comparison for Trinidad Head, CA, Kelowna, BC, Bratts Lake, SK, and Richland, WA.

These time-series indicate that both the TTOR and the Aura-ASM capture the general patterns measured by the ozonesondes. On average, the TTOR data were 13.8% below the ozonesonde column measurements, whereas Aura-ASM had an average percent difference of -0.8%. The precision of individual ozonesondes is 5% for measurement of partial pressure in the atmosphere (Thompson et al., 2003; Smit et al., 2007). Our percent differences for the Aura-ASM and TTOR 1.4 data products are slightly lower than differences obtained in previous works (Stajner et al., 2008; Schoeberl et al., 2007), which may be partly due to the relatively small spatial and time scales used in this analysis; or that Schoeberl et al. (2007) and Hui (2008) used version 1.3 of TTOR. Improvement of the cloud-resolving algorithm in TTOR 1.4 (Schoeberl - Personal Communication) increased

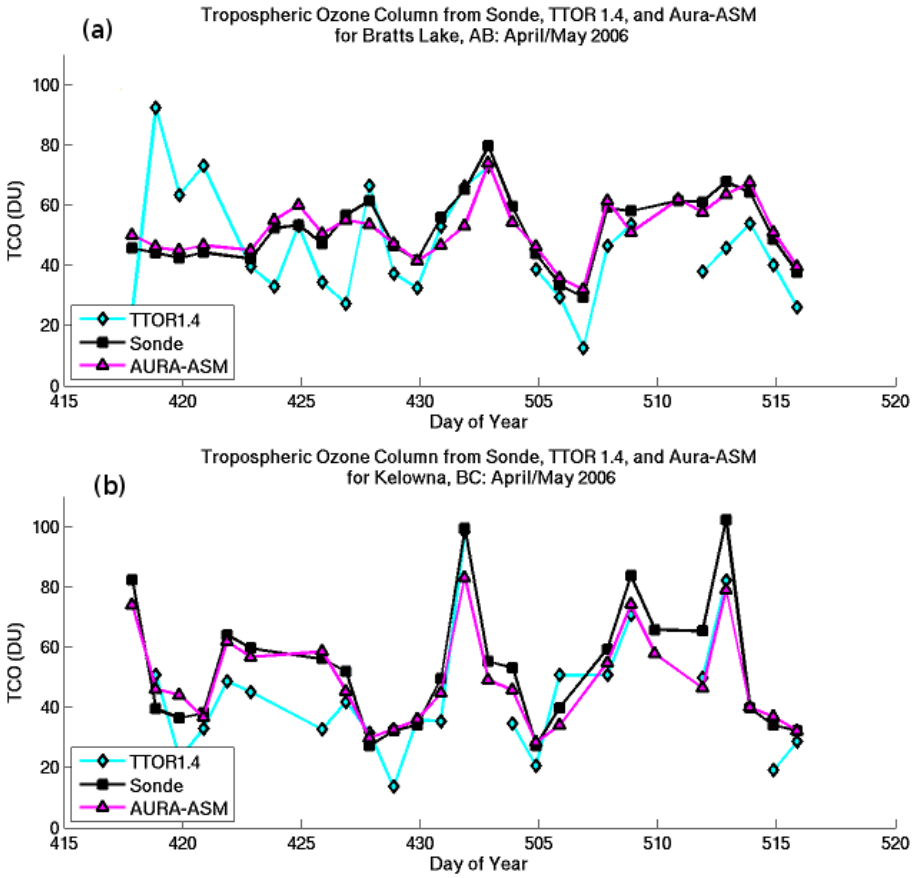

Figure 3.1. Time Series for surface to 200 hPa integrated column ozone at two Canadian locations during the Spring of 2006. Locations are (a)Bratts Lake, SK and (b) Kelowna, BC. 420 represents 4/20 or April 20.

data density which may partially account for the discrepancy. Average percent differences for the spring of 2006 for all four sites used in this study are given in Table 3.1.

Although the average percent differences show some variations, further analysis is needed to understand these variations in the performance of the data products. The data suggest that Aura-ASM provides significantly higher accuracy at all four study locations; however, both data products have similar errors at Trinidad Head. These errors are the subject of Case Study 1 in Chapter 4, where we illustrate that the ozone retrieval in the upper troposphere was biased high, leading to tropospheric ozone biases above 20 DU. This high bias counterbalanced the tendency of both data products to underestimate ozone lower in the troposphere.

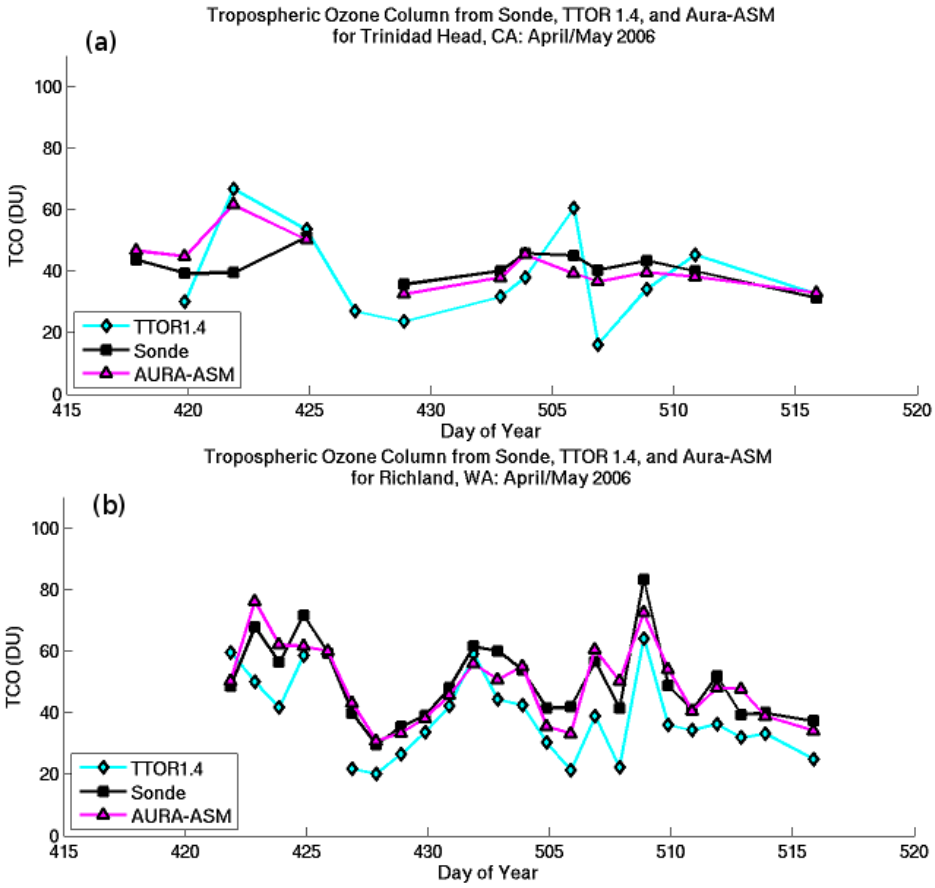

Figure 3.2. Time Series for surface to 200 hPa integrated column ozone at two US locations during the Spring of 2006. Locations are as follows (a):Trinidad Head, CA; (b):Richland, WA. 420 represents 4/20 or April 20.

	Trinidad Head	Kelowna	Brattslake	Richland	Avg
# Days	12	25	27	24	22
TTOR1.4	-4.7	-17.2	-9.6	-23.8	-13.8
AURA-ASM	2.5	-4.4	-0.3	-0.8	-0.7

Table 3.1. Mean percent differences between Aura-ASM/TTOR 1.4 and ozonesonde tropospheric integrated ozone from the surface to 200 hPa at four IONS-06 locations.

When this day is removed, the average mean percent difference for TTOR at Trinidad Head changed from -4.7% to -12%, and from 2.5% to -2.3% for Aura-ASM. This changed mean percent differences over all locations to -15.7% for TTOR and -1.9% for Aura-ASM. The Aura-ASM data appears to represent a significant improvement over TTOR, but Aura-ASM's small error is partly due to cancellation of low and high biases in the ozone profile as will be shown in the next section.

Error histograms, generated by subtracting ozonesonde tropospheric ozone from Aura-ASM or TTOR tropospheric ozone, are shown in Figures 3.3 and 3.4. These figures show slightly skewed distributions for both data products over most locations, with the Aura-ASM distribution slightly narrower than the TTOR one. Therefore, one must be careful in applying simple statistics to these data products. Additionally, error distributions varied greatly among the different locations. For example, the spread of the retrieval errors at Trinidad Head and Bratts Lake are larger than Richland and Kelowna. This is a surprising result, as one might expect the Kelowna measurements to vary more due to mountain wave generation and the more complex dynamics found at northern latitudes during the late spring (Creilson et al., 2003; Pierce and Grant, 1998). However, some have noted increased satellite resolution at higher altitudes that may be able to account for the smaller spread at Kelowna (Thompson et al., 2003).

3.2 Tropospheric Ozone Vertical Profiles

Because twelve of the Aura-ASM layers are in the troposphere (Table 3.2), we were able to examine ozone profiles in the troposphere and look at fine atmospheric structure. Recall that the average percent difference between ozonesondes and Aura-ASM is -1.9%.

Figures 3.5 a,c and 3.6 a,c show example ozonesonde soundings and AURA-ASM retrievals, and Fig. 3.5 b,d and Fig. 3.6 b,d show mixing ratio percent differences at the middle of each Aura-ASM pressure level. Mean in-situ ozone mixing ratios were calculated for each Aura-ASM pressure level, then compared to the Aura-ASM retrievals for all days in our study.

The profile percent-error graphs in Figs. 3.5 and 3.6 indicate that the AURA-ASM data product fluctuates between negative and positive biases. Except at

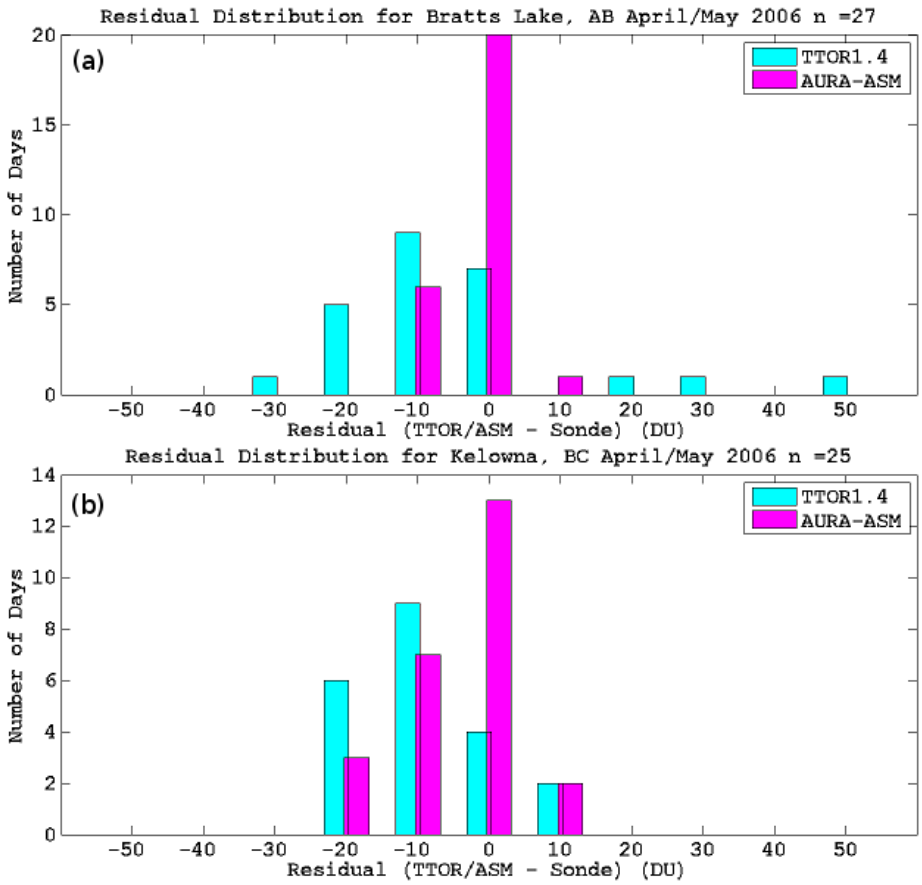

Figure 3.3. Histograms of surface to 200 hPa integrated column ozone errors for two Canadian IONS-06 sites.

Kelowna, biases are negative in the lower troposphere, positive in the middle to upper troposphere, and typically become negative above 200 hPa. When column integration is performed, these positive and negative biases cancel and produce high accuracy.

Figures 3.5 and 3.6 also provide context for the column integration height of 200 hPa. At the northernmost sites (Kelowna and Bratts Lake) the location of the mean dynamical tropopause is below the 200 hPa integration height, whereas the Trinidad Head and Richland mean dynamical tropopauses lie above and at 200 hPa, respectively. At all four locations, Aura-ASM has a positive bias between 300 and 200 hPa. This systematic bias was noted by Stajner et al. (2008), and illustrates one advantage of the static 200 hPa tropopause. Since the average dynamical

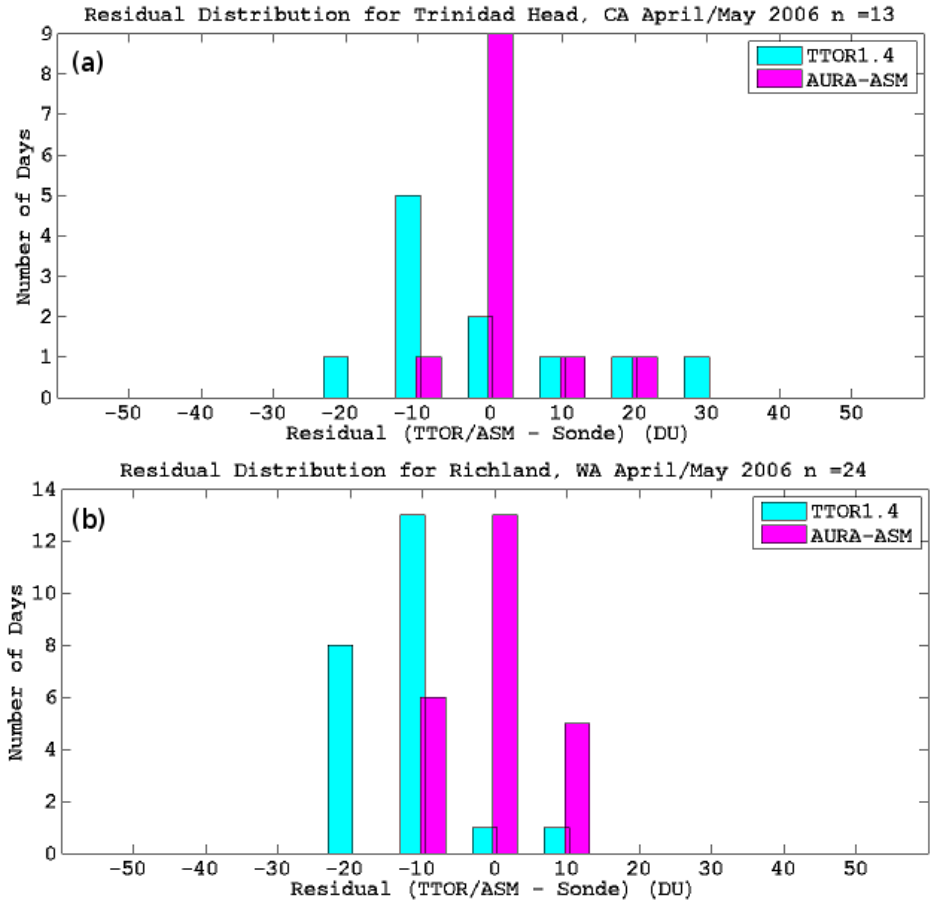

Figure 3.4. Histograms of surface to 200 hPa integrated column ozone errors for two US IONS-06 sites.

tropopause is located below 200 hPa at the more northerly sites, tropospheric ozone column integration to the dynamical tropopause not include much of this high-biased layer. At the southern sites, especially Trinidad Head, integration to the dynamical tropopause would include would this high biased data layer, introducing additional bias. Therefore, while using a lapse-rate or dynamic tropopause for our integration height may have avoided inclusion of stratospheric air in an integration, it would have introduced additional problematic issues.

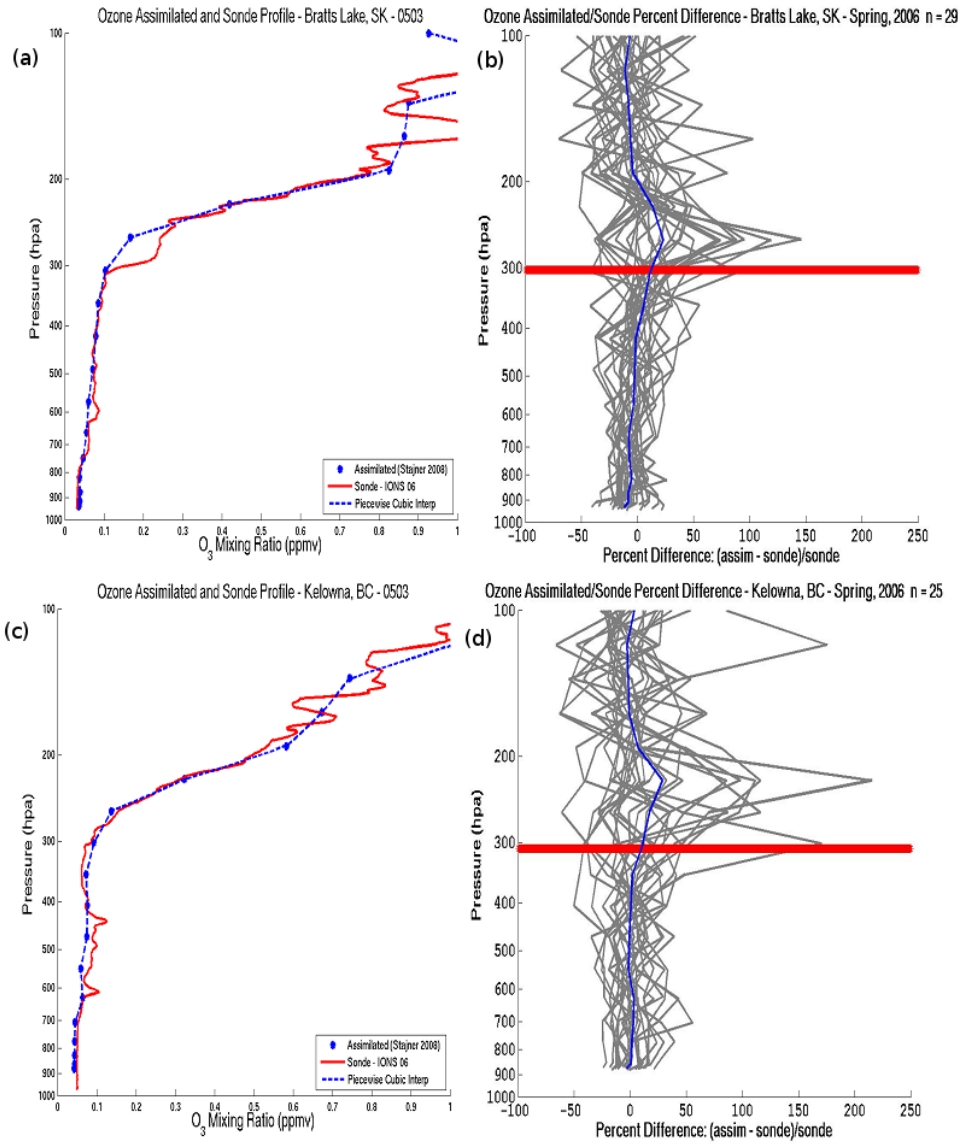

Figure 3.5. (a) and (c) show Canada ozonesonde pressure profiles for May 3, 2006, in red. Blue dots represent Aura-ASM ozone at the center of each model layer for 21z on May 3,2006, and are connected by a linear interpolation for visualization purposes. Percent differences between Aura-ASM and ozonesonde for each day of the study period were computed at each Aura-ASM pressure level by using average ozonesonde mixing ratios over each pressure level, and are shown in (b) and (d) in gray. The average percent differences over all days are shown by the blue lines. The red bars represent the average dynamic tropopause heights.

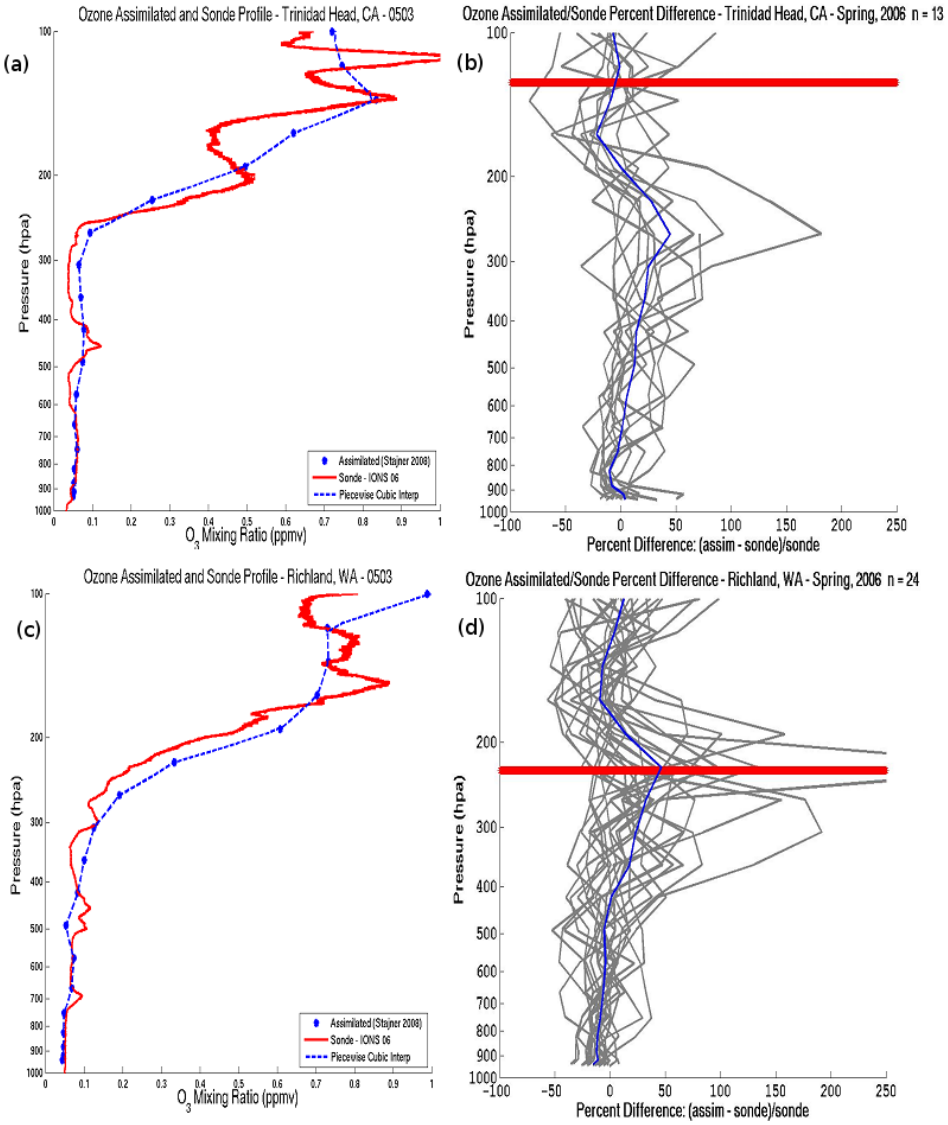

Figure 3.6. (a) and (c) show United States ozonesonde pressure profiles for May 3, 2006, in red. Blue dots represent Aura-ASM ozone at the center of each model layer for 21z on May 3,2006, and are connected by a linear interpolation for visualization purposes. Percent differences between Aura-ASM and ozonesonde for each day of the study period were computed at each Aura-ASM pressure level by using average ozonesonde mixing ratios over each pressure level, and are shown in (b) and (d) in gray. The average percent differences over all days are shown by the blue lines. The red bars represent the average dynamic tropopause heights.

Brattslake	Kelowna	Richland	Trinidad Head
937.3	878.49	935.16	970.32
916.8	859.68	914.73	948.88
878.92	825.3	876.97	909.03
821.06	772.77	819.3	848.17
747.47	705.9	745.96	770.81
663.26	629.27	662.02	682.34
574.03	547.92	573.08	588.69
490.91	471.87	490.22	501.59
420	406.71	419.51	427.45
359.43	350.72	359.11	364.32
307.59	302.4	307.4	310.51
263.12	260.48	263.02	264.6
224.84	223.85	224.8	225.39
191.73	191.54	191.72	191.84
163.12	163.12	163.12	163.12
138.66	138.66	138.66	138.66
117.86	117.86	117.86	117.86
100.18	100.18	100.18	100.18

Table 3.2. Aura-ASM average pressure levels at each IONS-06 location. Note that the last four pressure levels are the same at all sites.

3.3 Total Ozone Column Comparison

The OMI instrument provides total ozone column measurements used for the TTOR 1.4 and AURA-ASM calculations. OMI-TOMS total ozone column retrievals were analyzed to determine if errors in these measurements are causing tropospheric column errors. To accomplish this, OMI total column ozone data were compared to total column ozone from ozonesondes. Errors in OMI total column ozone are then compared to errors in tropospheric column ozone derived from both data products (Fig. 3.7). While TTOR and Aura-ASM errors range from about 0% to 80% and 0 to 40 %,respectively, all errors for OMI total ozone columns are less than 8% and appear to be uncorrelated to TTOR and Aura-ASM tropospheric column ozone errors, which suggests that OMI errors are not playing a significant role in tropospheric ozone retrieval errors.

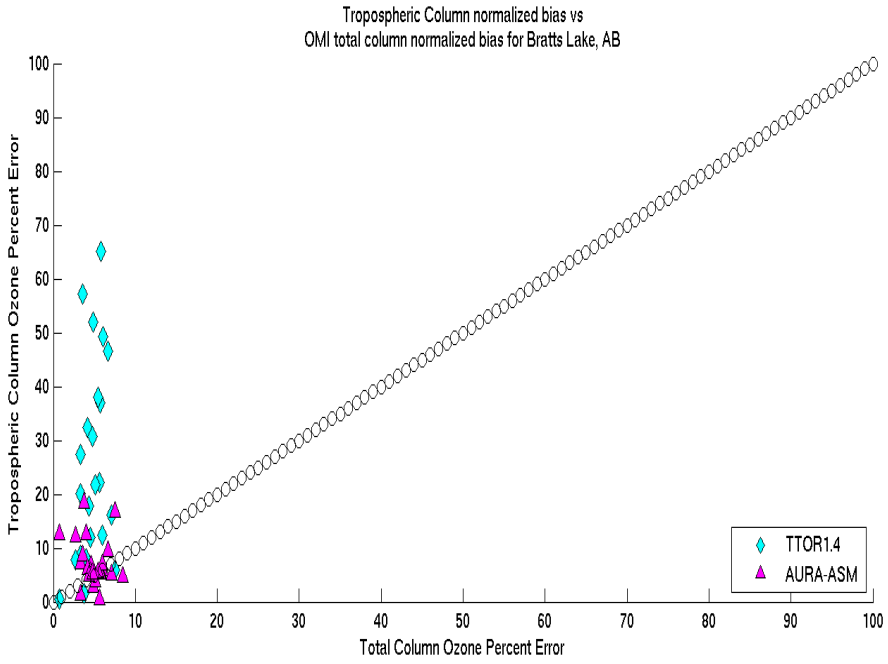

Figure 3.7. Total column ozone percent differences (compared with Ozonesonde values) versus tropospheric column ozone percent errors(Compared with ozonesonde values) for individual days at Bratts Lake, SK. Other locations exhibited similar behavior and are not shown.

Chapter 4

Aura-ASM/Sonde errors: Three case studies

When conducting a validation of satellite products, there are several sources of systematic error. The previous chapter discussed the distribution of errors. It also examined how positive biases could balance negative biases if averaged over a time-series. This chapter will review errors due to the pixel size of the AURA data and will examine case studies to investigate causes of errors in the Aura-ASM product. Case one covers a situation where no significant errors occured even in the presence of an upper level trough. Case two examines a situation where a trough is the likely cause of bifurcation in ozone concentration at adjacent Aura-ASM grid squares. Finally, case three examines the April 21 Trinidad Head comparision that represented a large enough discrepancy with the sondes and significantly impacted mean percent differences as presented in the previous chapter.

4.1 Pixel Areas

One potential source of error in our comparisons is the spatial resolution of the Aura-ASM and TTOR products, because the point measurements of ozonesondes are compared to the 1.25° by 1.00° grid size of the AURA-ASM and TTOR products. At Trinidad Head pixel size is 111 km by 105 km, whereas at Bratts Lake pixel size is 111 km by 83 km. Since ozone correlation length in the troposphere is 500-1000 km (Liu et al., 2009), one potential method to address spatial resolu-

tion differences is to determine the ozone value at the nearest four pixels to the ozonesonde launch point and then linearly interpolate to the coordinates of the ozonesonde launch location. This also has the side effect of accounting for any sonde drift.

After performing this interpolation at all sites, we did not find any significant changes in our comparisons. Additionally, we were concerned that the interpolation might mask dynamical features and introduce additional biases. For these two reasons, all figures and statistics shown in this thesis, unless otherwise noted, use the grid-square that contained the sonde launch point.

To examine any additional information that may be available in the Aura-ASM product at adjacent pixels, we plotted ozone profiles for all pixels adjacent to the one containing the sonde launch point. Fig. 4.1 shows an example of this plot where the Aura-ASM grid square that contains the sonde launch did not adequately resolve the features measured by the ozonesonde. The east, northeast, and north locations resolve the measured ozone profile better than the grid square containing the sonde launch. A look at the synoptic conditions for 18:00Z on this day indicates a significant geopotential height gradient to the north of this area, which may account for the observed difference. This adjacent pixel analysis proves to be useful when examining other difficult cases and will be an important technique as we examine several cases of the Aura-ASM retrieval, especially because it allows us to observe if meteorological variability is affecting the Aura-ASM retrieval.

4.2 Case Studies

The main motivation behind the case studies is to better understand factors that may cause errors seen in Aura-ASM profile retrievals (Figs. 3.5 and 3.6), initially focusing on synoptic conditions. Varying meteorological conditions have the potential to affect satellite retrievals and can also cause difficulty for models, especially if the model has a low resolution. However, there are other factors that may play a role in creating differences between Aura-ASM retrievals and ozonesonde measurements. To understand the role of meteorological conditions and other factors, we examine three cases that show similar meteorological conditions, but very different discrepancies between Aura-ASM retrievals and ozonesonde measurements.

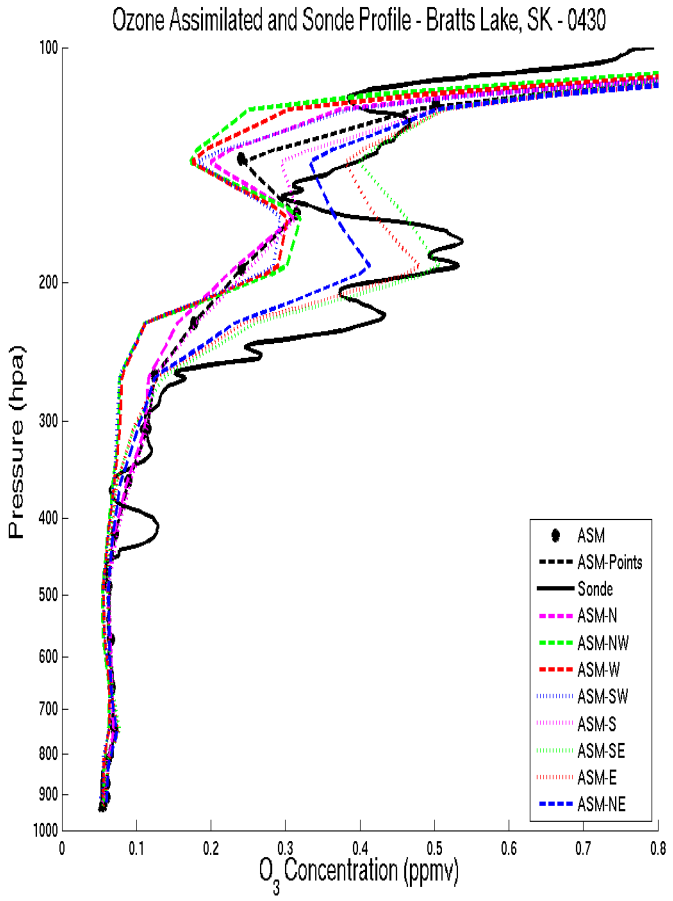

Figure 4.1. This plot shows all Aura-ASM pixels adjacent to and including the Aura-ASM pixel containing the sonde launch. Also shown is ozonesonde measurement (solid black line) Note that Aura-ASM pixel containing sonde launch does not reflect upper tropospheric features as well as several adjacent pixels, as described in section 4.1

4.2.1 Case Study 1: 2-3 May, 2006

The objective of this case study is to examine a period when the Aura-ASM exhibit typical performance (see Figs. 3.1 and 3.2) during the passage of a significant trough. We look at May 2-3, when a trough is deepening over the western US and a cutoff low is forming over Saskatchewan and Manitoba, e.g, Figs. 4.2. During this time, tropopause height is declining over the US, which can be seen in Fig. 4.2 as the 250 hPa tropopause (pink line) extends farther south on May 3 than it did the previous day.

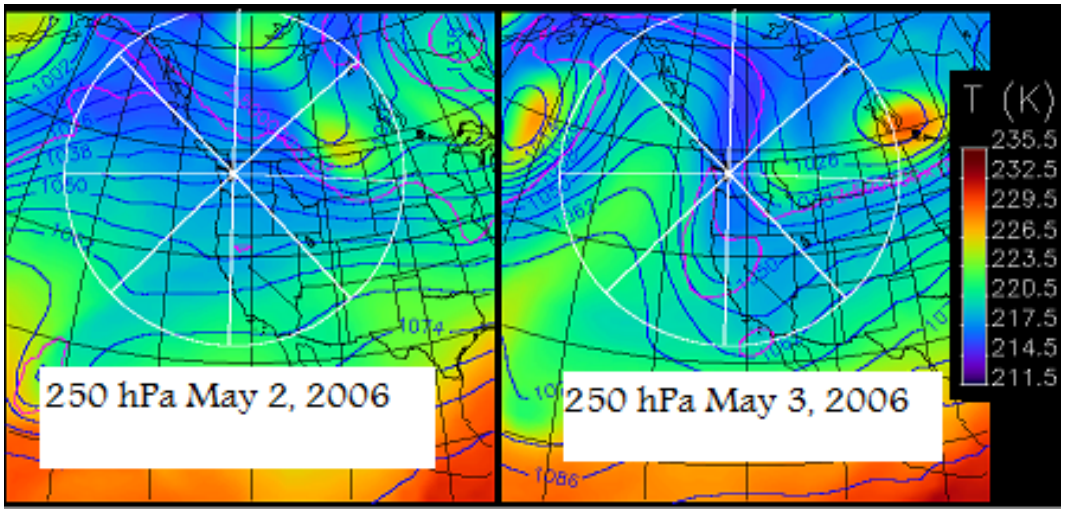

Figure 4.2. GEOS-4 250 hPa heights for May 2 and 3 at Bratts Lake, SK at 18 Z. Blue lines correspond to geopotential height in decameters, colors to temperature, and the pink line represents the location where the tropopause is at 250 hPa. GEOS data from: http://croc/gsfc/nasa/gov/intex/IMAGES/CP

The Richland soundings show several interesting features at this time. On May 2 (Fig. 4.3), the Richland Aura-ASM profile approximates the tropopause height and upper tropospheric ozone. This day had a north-south geopotential height gradient at 250 hPa. Over the following 24 hours from May 2 to May 3, a trough deepened over the west coast. This began to decrease geopotential heights, especially at more southerly locations like Trinidad Head. At Richland, the tropopause region on May 3 could arguably be placed at a slightly higher altitude due to the ridge building off the west coast, but the Aura-ASM product slightly underestimates this height. This suggests that Aura-ASM retrievals may have some difficulty in the presence of height gradients. We will examine this effect further in the following two case studies.

Finally, note the spikes in ozone concentration at 700 hPa and 300-500 hPa on both May 2 and 3 in the Richland, WA, profiles. Are these spikes (which are unresolved by the model) related to intrusions of high ozone stratospheric air into the troposphere? Laminar Identification Analysis (LID) (Thompson et al., 2007; Dougherty, 2008; Luzik, 2009), which budgets ozone into several sources, suggests that they are due to other factors. In summary, we do not observe any significant

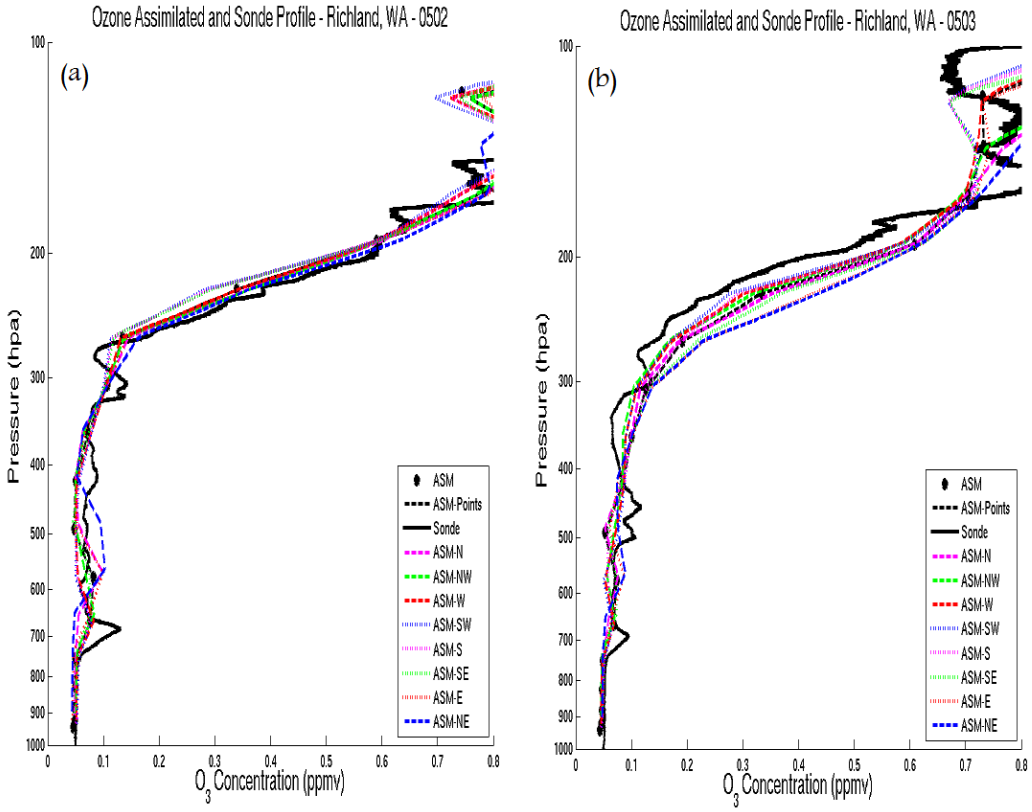

Figure 4.3. Aura-ASM and ozonesonde profiles from Richland, WA, for May 2 and 3, 2006. Solid black line shows the ozonesonde profile and the dashed black line shows Aura-ASM retrieval from the pixel containing the launch site. All other lines come from adjacent pixels, as described in the legend.

retrieval errors on May 2 or 3, although Aura-ASM retrievals have minor difficulty resolving upper troposphere ozone and middle troposphere ozone spikes during the presence of a front.

4.2.2 Case Study 2: 17 April, 2006

The previous case study illustrated that under the steep height gradients observed with the trough on May 3, there was a slight overprediction of ozone. In this second case study, which examines Bratts Lake profiles from April 17, 2006, we examine further the performance of the Aura-ASM retrieval when under strong geopotential height gradients. Figure 4.4 shows synoptic conditions at Bratts Lake

on April 17th. These are similar to those observed at Richland on May 3 - a deep trough is near the study site along with steep geopotential height gradients.

Examination of the ozone profile for this day reveals two interesting features(Fig. 4.5). First, a high bias in the Aura-ASM retrieval is present from 250 to 200 hPa. Recall in Chapter 3 that we discussed the persistent high bias in this range. We have observed it in case studies 1 and 2. Second, there is a bifurcation in ozone in the upper troposphere/lower stratosphere (Fig. 4.5). At pressures near and slightly below 200 hPa, the pixel containing the ozonesonde launch, as well as pixels to the northeast, east, southeast, and south, display the Aura-ASM retrievals with ozone mixing ratios 100 ppbv below that of the sondes, with southeast having the greatest discrepancy. The other pixels had profiles that were close to the sonde mixing ratios, with the northwest overestimating ozone by the highest amount. An examination of the dynamic conditions at 250 hPa shows strong geopotential height gradients from northwest to southeast; these persist to 100 hPa.

Because both the gradient in geopotential height at 250 hPa is northwest to southeast and the gradient in overestimation/underestimation of ozone is northwest to southeast, we infer that this is a case when the dynamical conditions are playing the dominant role leading to the differences in ozone profiles. Further research should incorporate statistical tools to characterize the performance of the Aura-ASM retrieval with different synoptic regimes. Some discrepancies between Aura-ASM and the ozonesondes cannot be explained merely by synoptic conditions.

4.2.3 Case Study 3: 21 April, 2006

On April 21, 2006, there is a significant ozone discrepancy between the Trinidad Head ozonesonde and the Aura-ASM retrievals (Figure 4.6). Both the AURA-ASM and the TTOR 1.4 retrievals indicate column ozone greater than 60 % above the ozonesonde surface to 200 hPa integration. The high percent difference on this day significantly changed the average percent differences over all 12 days of the campaign(see section 3.2). When this day is removed, Trinidad Head average percent errors are much closer to the percent errors observed at the other locations.

As in the previous two case studies, we first examine the meteorological condi-

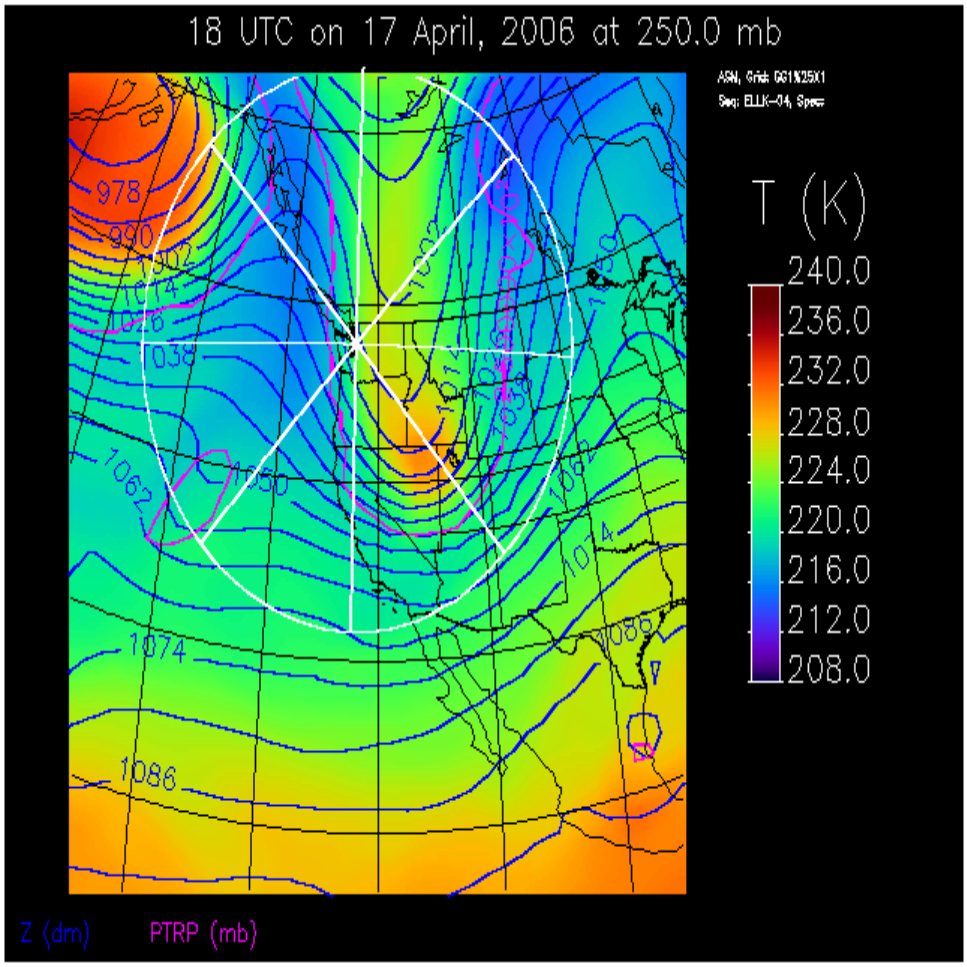

Figure 4.4. GEOS-4 atmospheric conditions at 250 HPa for Richland, WA, at 18:00Z on April 17, 2006. Blue ines correspond to geopotential height in decameters, colors to temperature, and the pink line represents the location where the tropopause is at 250 hPa. GEOS data from: http://croc/gsfc/nasa/gov/intex/IMAGES/CP.

tions to determine if dynamics the source of this discrepancy. There is an upper level trough approaching the west coast of the United States, and Trinidad Head is near the center of that trough (Fig. 4.7). An examination of the profile shows that, while there is a slight northeast/southwest progression in ozone mixing ratios in the upper troposphere, all Aura-ASM retrievals at and surrounding the pixel containing the Trinidad Head the ozonesonde launch have significant differences with ozonesonde mixing ratios. This suggests other sources of variation than simply the large-scale synoptic dynamics that we saw in previous case studies.

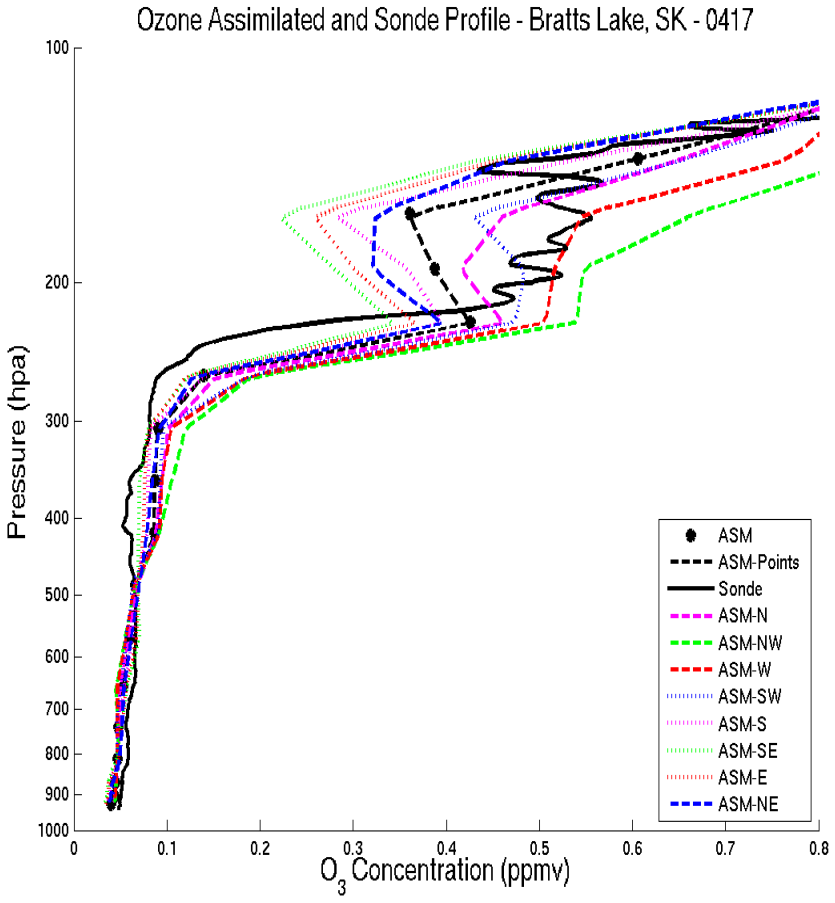

Figure 4.5. Profiles for Bratts Lake on April 17, 2006. Solid black line shows ozonesonde profile, dashed black line shows Aura-ASM retrieval from the pixel containing the launch site. All other lines come from adjacent pixels, as described in the legend.

We examined other potential causes of the difference. The in-situ ozonesonde data were examined to verify the accuracy of our "truth". The sonde for this day exhibited extremely low ozone pump current, suggesting that there may be abnormal ozone measurements, especially at high altitudes. However, data are still acceptable up to around 18 km, well above our 200 hPa integration height (Oltmans, 2009).

We also considered that the assimilation time may have been causing our differences. The assimilations are produced every three hours. For all of our comparisons, we compared the 21:00Z assimilation, which is approximatly the launch time

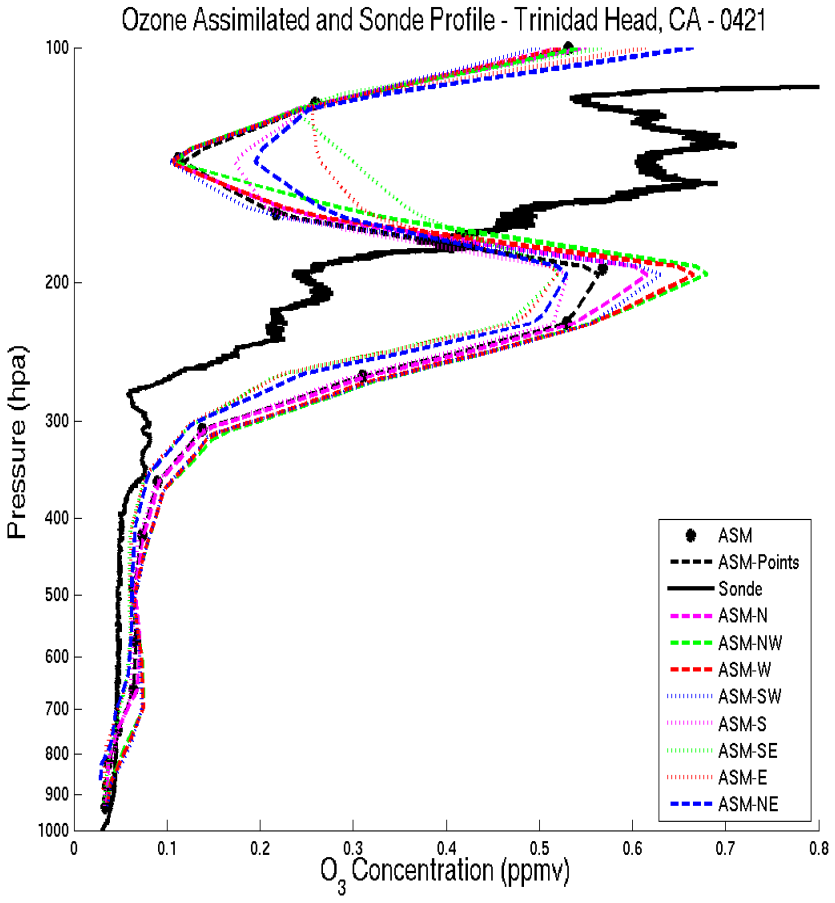

Figure 4.6. Profiles for Trinidad Head on April 21, 2006. Solid black line shows ozonesonde profile, dashed black line shows Aura-ASM retrieval from the pixel containing the launch site. All other lines come from adjacent pixels, as described in the legend.

of most sondes. On this day, the sonde was launched at 20:28Z, and we also examined the assimilations from three hours before and after 21:00Z to make sure that assimilation time was not playing a role in our analysis (Fig. 4.8). While changing the assimilation time does not decrease the low prediction of ozone around 150 hPa, the 00:00Z assimilation does show close approximation between the sonde and Aura-ASM ozone concentration at 200 hPa. Thus, assimilation time may have had a role in this case, although it does not explain the persistence of the low estimates at 150 hPa. In order to determine if there is a relationship between assimilation time and sonde/Aura-ASM ozone concentration agreement, we will need to exam-

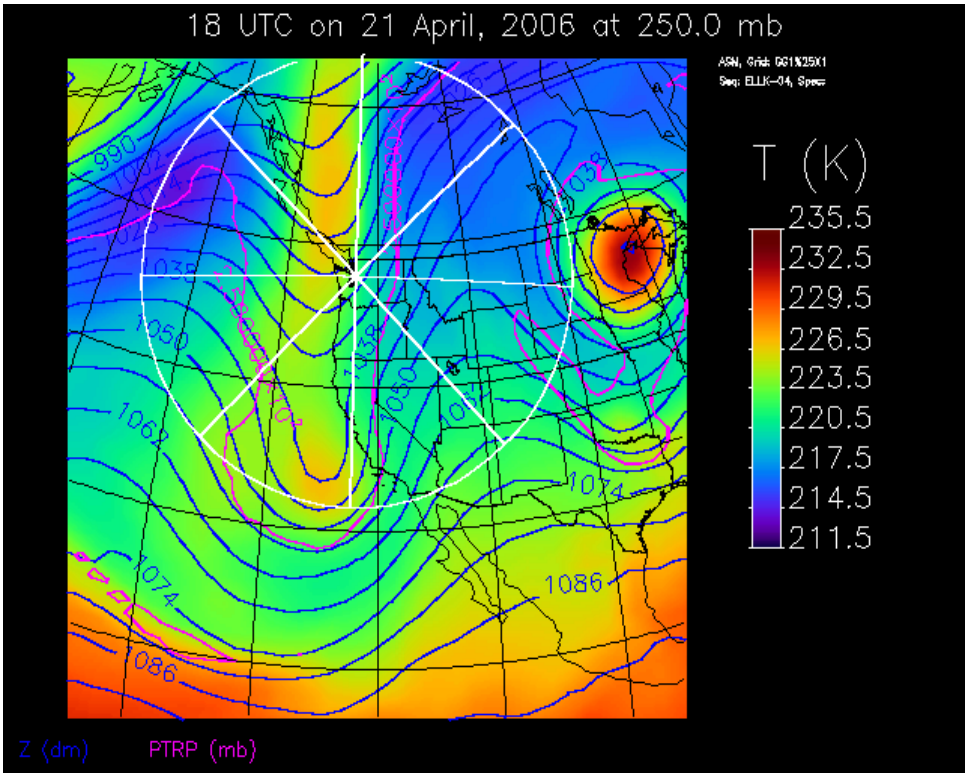

Figure 4.7. GEOS-4 atmospheric conditions at 250 HPa heights for Trinidad Head, CA on April 21 at 18Z. Blue lines correspond to geopotential height in decameters, colors to temperature, and the pink line represents the location where the tropopause is at 250 hPa. GEOS data from: http://croc/gsfc/nasa/gov/intex/IMAGES/CP

ine raw MLS data and Aura overpass times, which would be an important part of any future work.

4.3 Summary

From the examination of case studies, we observed some variability in the Aura-ASM data product near fronts. This was expected, as the Aura-ASM product has a limited spatial resolution, and so might not be able to resolve all the ozone features near the environs at a front, although this variability might better be understood by a statistical analysis of meteorological conditions encountered during the campaign. Additionally, since differences in time between model assimilation and sonde launches appear to have had an effect in Case 3, we observed that fronts

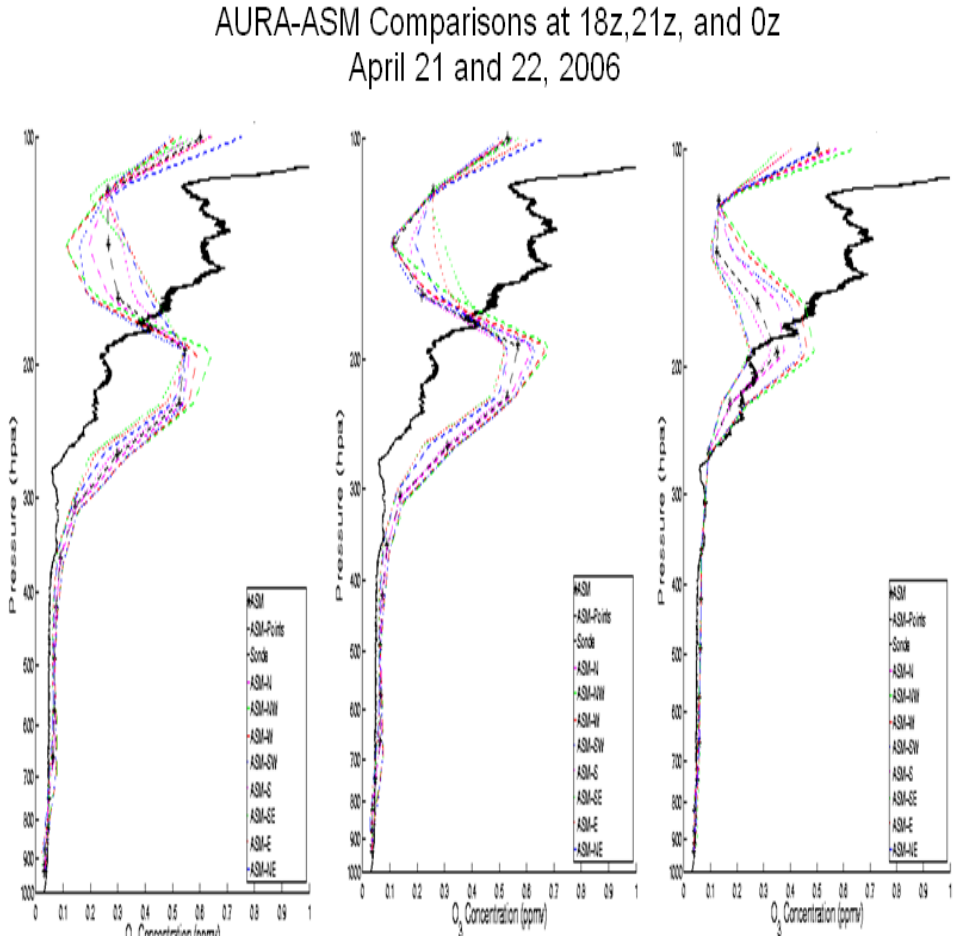

Figure 4.8. Progression of AURA-ASM retrievals for three output times. Black dashed line indicates the pixel that contains sonde launch, other lines indicate adjacent pixels. From left to right, 18z Apr. 21, 21z Apr. 21, 00z, Apr. 22

and dynamical variability do not appear to explain all major differences between the Aura-ASM product and the ozonesonde measurements. Thus, future work should incorporate MLS data and Aura-overpass times into the analysis.

Chapter 5

Summary, Conclusions, and Future Research

There have been many improvements to satellite retrievals of ozone in the troposphere. Results from two current methods, a tropospheric ozone residual method and a data assimilation method were compared to in-situ ozonesonde measurements. The average error for the Trajectory Enhanced Tropospheric Ozone Residual (TTOR) was -15.7%, and the average error for the OMI/MLS Assimilation (AURA-ASM) was -1.9%. We observed that the low error for the AURA-ASM product is partially due to systematic cancellation of errors in the troposphere and stratosphere, with some heights usually biased high and others biased low. Errors did not appear to be due to OMI-TOMS total ozone column retrieval errors.

Additionally, several cases in Spring, 2006 were examined to better understand the effect of dynamics on the ability of Aura-ASM and TTOR to resolve tropospheric ozone. In the case of May 2-3 at Richland, WA, we observed the impact of normal geopotential height gradients where the AURA-ASM product closely matches the in-situ retrieval. April 17 at Bratts Lake, SK, amplifies this observation by showing how one retrieval had difficulty because the Aura-ASM profile in the pixel containing the sonde launch location does not capture the dynamical variations within the atmosphere. April 21 at Trinidad Head, CA, showed a problematic retrieval where errors are not simply related to the passage of a front, but may be due to MLS satellite retrieval problems, ozonesonde measurement error, Aura-ASM retrieval time, or an atmospheric feature not resolved by the model.

These three case studies illustrate the questions that remain about the performance of the Aura-ASM data product. While one might expect some variability in the region of fronts, dynamics do not completely explain some of the case studiies, such as what was observed the 21st of April, so other factors are evidently at work.

Several areas remain ripe for further research. First, analysis of MLS data would greatly improve our error analysis, as it is a significant independent variable, with errors at 215 hPa reaching 20% (Froidevaux et al., 2008). This will not be a simple task, as the MLS level 2 data are only available in swaths. MLS data combined with the OMI data that were analyzed in this thesis will offer a more complete picture of factors that affect the OMI/MLS assimilation and TTOR accuracy.

Also, since the IONS-06 intensive campaign included additional locations at other latitudes, such as Stony Plain, AB, and Houston, TX, these sites can be analyzed to better understand chemical relationships. For example, Houston is well known for its high amounts of air pollution. Analysis of Houston data could clarify the ability of the assimilation to resolve chemistry.

Finally, several studies (Thompson et al., 2007; Luzik, 2009; Yorks et al., 2009) have used analysis of ozone laminae in IONS ozonesondes to partition tropospheric ozone into four sources: boundary layer, stratosphere, regional convection/lightning, and "other" (mostly due to long-distance transport). It is possible to use this information to understand more about these satellite data products. An analysis of variance (ANOVA) could be used to compare the performance of TTOR and Aura-ASM under different ozone forcings, and determine which method is most sensitive to various ozone sources. This goes beyond simple validation and begins to examine the physical basis of both methods.

This is the ultimate goal of any validation. As the OMI data user guide (OMI, 2009) states "validation is never over". In the ongoing quest to improve our knowledge of tropospheric ozone, both of these data products offer improvements over previous ones.

Appendix A

Selected Acronyms

OMI : Ozone Monitoring Instrument, one of the four instruments onboard the AURA satellite

MLS : Microwave Limb Sounder, one of the four instruments onboard the Aura Satellite

ECC : Electrochemical concentration cell, a type of ozonesonde commonly used at many sites around the world

UV : Ultraviolet Light, in the atmosphere, relevant wavelengths are between 200nm and 400nm

UTLS : Upper Troposphere/Lower Stratosphere, this region of the atmosphere presentes difficulty for many models due to its dynamical complexity and high gradients in temperature and potential vorticity

SBUV : Solar Backscattered Ultraviolet limb sounder that made stratospheric measurements

SCO: Stratospheric Column Ozone

PV: Potential vorticity, proportional to the dot product of vorticity and straification (Holton, 2004).

CCD: Convective Cloud Differential

SAGE : Stratospheric Aerosols and Gases Experiment: The first satellite to make "stratospheric ozone" measurements using solar occultation

TOC : Total Ozone Column - The total amount of ozone in a vertical column above a 1cm by 1cm square

DU : Dobson Unit, a unit of integrated ozone. It is the depth of ozone in

hundredths of a millimeter if a ll the ozone in a layer were brought to STP. 1 Dobson Unit is approximately equal to 10^{16} molecules of ozone

TOR : Tropospheric Ozone Residual - Tropospheric Ozone Column data retrieved by subtracting stratospheric ozone column from total ozone column

TTOR : Trajectory-Enhanced Tropospheric Ozone Residual, improves Tropospheric Ozone Residuals by using Trajectories to spread stratospheric ozone retrievals over the globe

GOES :Geostationary Operational Environmental Satellite

GEOS : Goddard Earth Observing System: A data assimilation system developed at the Goddard Space Flight Center.

GCM : General Circulation Model

Bibliography

D. Balis, M. Kroon, M. Koukouli, E. Brinksma, G. Labow, J. Veefkind, and R. McPeters. Validation of ozone monitoring instrument total ozone column measurements using brewer and dobson spectrophotometer ground-based observations. *Journal of Geophysical Research*, 112, 2007. doi: 10.1029/2007JD008796.

S. Bloom, A. da Silva, and D. Dee. Documentation and validation of the goddard earth observing system (geos) data assimilation system - version 4. Technical report, Goddard Space Flight Center, 2005.

I. Boyd, A. Parrish, L. Froidevaux, T. von Clarmann, E. Kyrölä, J. Russell, and J. Zawodny. Ground-based microwave ozone radiometer measurements compared with aura-mls v2.2 and other instruments at two network for detection of atmospheric composition sites. *Journal of Geophysical Research*, 112, 2007. doi: 10.1029/2007JD008720.

J. Creilson, J. Fishman, and A. Wozniak. Intercontinental transport of tropospheric ozone: a study of its seasonal variability across the north atlantic utilizing tropospheric ozone residuals and its relationship to the north atlantic oscillation. *Atmospheric Chemistry and Physics*, 3:2053–2056, 2003.

G.M.B. Dobson. A photoelectric spectrophotometer for measuring the amount of atmospheric ozone. *Proceedings of the Physical Society*, 43:324–339, 1931.

G.M.B. Dobson. Forty years' research on atmospheric ozone at oxford. *Applied Optics*, 7(3):387–405, March 1968.

M. Dougherty. The effect of ozonopause placement on tropospheric ozone budgets: An analysis of ozonesonde profiles from selected ions-06 sites. Master's thesis, The Pennsylvania State University, 2008.

E. Fiscus, F. Booker, and K. Burkey. Crop responses to ozone: Uptake, modes of action, carbon assimilation and partitioning. *Plant, Cell, and Environment*, 28: 997–2011, 2005.

J. Fishman and V. Brackett. The climatological distribution of tropospheric ozone derived from satellite measurements using version 7 total ozone mapping spectrometer and stratospheric aerosol and gas experiment data sets. *Journal of Geophysical Research*, 102(D15), August 1997.

J. Fishman, C. Watson, J. Larsen, and J. Logan. Distribution of tropospheric ozone determined from satellite data. *Journal of Geophysical Research*, 95(D4): 3599–3617, March 1990.

J. Fishman, J. Creilson, A. Wozniak, and P. Crutzen. Interannual variability of stratospheric and tropospheric ozone determined from satellite measurements. *Journal of Geophysical Research*, 110, 2005. doi: 10.1029/2005JD005868.

L. Froidevaux, Y. Jiang, A. Lambert, N. Livesey, W. Read, J. Waters, E. Browell, J. Hair, M. Avery, T. McGee, L. Twigg, G. Sumnicht, and K. et al. Jucks. Validation of aura microwave limb sounder stratospheric ozone measurements. *Journal of Geophysical Research*, 2008. doi: 10.1029/2007JD008771.

F. Gotz, A. Meetham, and G. Dobson. The vertical distribution of ozone in the atmosphere. *Proceedings of the Royal Society of London*, 145(855):416–436, July 1934.

W.C.J. Hui. Comparison of ozone measurements by satellite, sondes, and other instruments over north america during the ions (2006) campaign. Master's thesis, The Pennsylvania State University, 2008.

W Komhyr. Electrochemical concentration cells for gas analysis. *Annales de Geophysique*, 24(1), 1969.

P. Levelt, G. van den Oord, M. Dobber, A. Mälkki, H. Visser, J. de Vries, P. Stammes, J. Lundell, and H. Saari. The ozone monitoring instrument. *IEEE Transactions on Geoscience and Remote Sensing*, 44(5):1093–1101, May 2006.

G. Liu, D. Tarasick, V. Fioletov, C. Sioris, and Y Rochon. Ozone correlation lengths and measurement uncertainties from analysis of historical ozonesonde data in north america and europe. *Journal of Geophysical Research*, 114, 2009. doi: 10.1029/2008JD010576.

A. M. Luzik. Quantifying forest fire enhancement of the free tropospheric ozone column during the ions-04, ions-06, and arc-ions campaigns. Master's thesis, The Pennsylvania State University, 2009.

M. Mccormick, P. Hamill, T. Pepin, W. Chu, T. Swissler, and L. McMaster. Satellite studies of the stratospheric aerosol. *Bulletin of the American Meteorological Society*, 60(9), 1979.

R. McPeters, M. Kroon, G. Labow, E. Brinksma, D. Balis, I. Petropavlov, J. Veefkind, P. Bhartia, and P. Levelt. Validation of the aura ozone monitoring instrument total column ozone product. *Journal of Geophysical Research*, 113: 1038–1046, May 2008.

Samuel Oltmans. personal communication, 2009.

Ozone Monitoring Instrument (OMI) Data User's Guide. OMI Team, March 2009.

B. Pierce and W. Grant. Seasonal evolution of rossby and gravity wave induced laminae in ozonesonde data obtained from wallops islane, virginia. *Geophysical Research Letters*, 25(11):1859–1862, June 1998.

M. Schoeberl, J. Ziemke, B. Bojkov, N. Livesey, B. Duncan, S. Strahan, L. Froidevaux, S. Kulawik, P. Bhartia, S. Chandra, P. Levelt, J. Witte, A. Thompson, E. Cuevas, A. Redondas, D. Tarasick, J. Davies, G. Bodeker, G. Hansen, B. Johnson, S. Oltmans, H. Voemel, M. Allaart, H. Kelder, M. Newchurch, S. Godin-Beekmann, G. Ancellet, H. Claude, S. Andersen, E. Kyroe, M. Parrondos, M. Yela, G. locki, D. Moore, H. Dier, P. von der Gathen, P. Witte, R. Stuebi, B. Calpini, P. Skrivankova, V. Dookhov, H. de Backer, F. J. Schmidlin, G. Coetzee, M. Fujiwara, V. Thouret, F. Posny, G. Morris, J. Merrill, C. P. Leong, G. Koenig-Langlo, and E. Joseph. A trajectory-based estimate of the tropospheric ozone column using the residual method. *Journal of Geophysical Research-Atmospheres*, 112, 2007. doi: 10.1029/2007JD008773.

H. Smit, W. Straeter, B. Johnson, S. Oltmans, J. Davies, D. Tarasick, B. Hoegger, R. Stubi, F. Schmidlin, T. Northam, A. Thompson, J. Witte, I. Boyd, and F. Posny. Assessment of the performance of ecc-ozonesondes under quasi-flight conditions in the environmental simulation chamber:insights from the juelich ozone sonde intercomparison experiment (josie). *Journal of Geophysical Research*, 112, 2007. doi: 10.1029/2006JD007308.

I. Stajner, K. Wargan, S. Pawson, H. Hayashi, L. Chang, R. Hudman, L. Froidevaux, N. Livesey, P. Levelt, A. Thompson, D. Tarasick, R. Stuebi, S. Andersen, Y Margarita, G. Koenig-Langlo, F. Schmidlin, and J. Witte. Assimilated ozone from eos-aura: Evaluation of the tropopause region and tropospheric columns. *Journal of Geophysical Research-Atmospheres*, 113, MAY 29 2008. doi: 10.1029/2007JD008863.

D. Tarasick, J. Jin, V. Fioletov, G. Liu, A. Thompson, and S. Oltmans. An ozone climatology for intex and arctas from ions ozonesondes. *Journal of Geophysical Research*, Submitted. doi: 2009JD013918.

A. Thompson, L. Sparling, Y. Kondo, B. Anderson, G. Gregory, and G. Sachse. Perspectives on no, noy, and fine aerosol sources and variability during sonex. *Geophysical Research Letters*, 26:3073–3076, 1999. doi: 10.1029/1999GL900581.

A. Thompson, J. Witte, R. McPeters, and et. al. Southern hemisphere additional ozonesondes(shadoz) 1998-2000 tropical ozone climatology 1. comparison with total ozone mapping spectrometer (toms) and ground-based measurements. *Journal of Geophysical Research*, 108, 2003. doi: 10.1029/2001JD000967.

A. Thompson, J. Stone, J. Witte, S. Miller, R. Pierce, R. Chatfield, S. Oltmans, O. Cooper, A. Loucks, B. Taubman, B. Johnson, E. Joseph, T. Kucsera, J. Merrill, G. Morris, S. Hersey, G. Forbes, M. Newchurch, F. Schmidlin, D. Tarasick, V. Thouret, and J. Cammas. Intercontinental chemical transport experiment ozonesonde network study (ions) 2004: 1. summertime upper troposphere/lower stratosphere ozone over northeastern north america. *Journal of Geophysical Research*, 112, 2007. doi: 10.1029/2006JD007441.

J. Waters, L. Froidevaux, R. Harwood, R. Jarnot, H. Pickett, W. Read, P. Siegel, R. Cofield, and et. Filipiak, M. al. The earth observing system microwave limb sounder (eos mls) on the aura satellite. *IEEE Transsactions on Geoscience and Remote Sensing*, 44(5):1075–1092, May 2006.

J. Yorks, A. Thompson, E. Jospeh, and S. Miller. The variability of free tropospheric ozone over beltsville, maryland (39n, 77w) in the summers 2004-2007. *Atmospheric Environment*, (43):1827–1838, 2009.